Hindawi
Advances in High Energy Physics
Volume 2021, Article ID 6645678, 22 pages
https://doi.org/10.1155/2021/6645678

Research Article

Confinement of Fermions in Tachyon Matter at Finite Temperature

Adamu Issifu,[1] **Julio C. M. Rocha**,[1] **and Francisco A. Brito**[1,2]

[1]*Departamento de Física, Universidade Federal da Paraíba, Caixa Postal 5008, 58051-970 João Pessoa, Paraíba, Brazil*
[2]*Departamento de Física, Universidade Federal de Campina, Grande Caixa Postal 10071, 58429-900 Campina Grande, Paraíba, Brazil*

Correspondence should be addressed to Francisco A. Brito; fabrito@df.ufcg.edu.br

Received 2 January 2021; Revised 13 February 2021; Accepted 7 April 2021; Published 5 May 2021

Academic Editor: Edward Sarkisyan Grinbaum

We study a phenomenological model that mimics the characteristics of QCD theory at finite temperature. The model involves fermions coupled with a modified Abelian gauge field in a tachyon matter. It reproduces some important QCD features such as confinement, deconfinement, chiral symmetry, and quark-gluon-plasma (QGP) phase transitions. The study may shed light on both light and heavy quark potentials and their string tensions. Flux tube and Cornell potentials are developed depending on the regime under consideration. Other confining properties such as scalar glueball mass, gluon mass, glueball-meson mixing states, and gluon and chiral condensates are exploited as well. The study is focused on two possible regimes, the ultraviolet (UV) and the infrared (IR) regimes.

1. Introduction

Confinement of heavy quark states $\bar{Q}Q$ is an important subject in both theoretical and experimental studies of high-temperature QCD matter and quark-gluon-plasma phase (QGP) [1]. The production of heavy quarkonia such as the fundamental state of $\bar{c}c$ in the Relativistic Heavy Iron Collider (RHIC) [2] and the Large Hadron Collider (LHC) [3] provides basics for the study of QGP. Lattice QCD simulations of quarkonium at finite temperature indicate that J/ψ may persist even at $T = 1.5T_c$ [4], i.e., a temperature beyond the deconfinement temperature. However, in simple models such as the one under consideration, confinement is obtained at $T < T_c$, deconfinement and QGP phase at $T \geq T_c$. Several approaches of finite temperature QCD have been studied over some period now, but the subject still remains opened because there is no proper understanding of how to consolidate the various different approaches [5–10]. Ever since, the Debye screening of heavy $\bar{Q}Q$ potential was put forward [11], leading to the suppression of quarkonia states such as J/ψ. Attention has been directed to investigations to understand the behavior of $\bar{Q}Q$ at the deconfined phase by nonrelativistic calculations [12–16] of the effective potential or lattice QCD calculations [4–8, 17].

We will study the behavior of light quarks such as up (u), down (d), and strange (s) quarks and also heavy quarks such as charm (c) and other heavier ones with temperature (T). We will elaborate on the net confining potential, vector potential, scalar potential energy, string tension, scalar glueball masses, glueball-meson mixing states, and gluon condensate with temperature. Additionally, confinement of quarks at a finite temperature is an important phenomenon for understanding the QGP phase. This phase of matter is believed to have formed few milliseconds after the Big Bang before binding to form protons and neutrons. Consequently, the study of this phase of matter is necessary for understanding the early universe. However, creating it in the laboratory poses a great challenge to physicists, because immensely high energy is needed to break the bond between hadrons to form free particles as it existed at the time. Also, the plasma, when formed, has a short lifetime, so they decay quickly to elude detection and analyses. Some theoretical work has been done

in tracing the signature of plasma formation in a series of heavy ion collisions. Nonetheless, a phenomenological model that throws light on the possible ways of creating this matter is necessary. In this model, the QGP is expected to be created at extremely high energy and density by regulating temperature, $T > T_c$. Besides these specific motivations for this paper, all others pointed out in [18, 19] are also relevant to this continuation. This paper is meant to complement the first two papers in this series [18, 19]. Particularly, it is a continuation of [18]. We will try as much as possible to maintain the notations in [18] in order to make it easy to connect the two. That notwithstanding, we will redefine some of the terms for better clarity to this paper when necessary. Generally, we will investigate how thermal fluctuations affect confinement of the fermions at various temperature distribution regimes. The Lagrangian adopted here has the same structure as the one used in [18], so we will not repeat the discussions.

Even though strong interactions are known to be born out of non-Abelian gauge field theory, no one has been able to compute confining potentials through this formalism. Therefore, several phenomenological models have been relied upon to describe this phenomenon. Common among which are linear and Cornell potential models. Bound states of heavy quarks form part of the most relevant parameters for understanding QCD in high-energy hadronic collisions together with the properties of QGP. As a result, several experimental groups such as CLEO, LEP, CDF, D0, Belle, and NA5 have produced data, and currently, ongoing experiments at BaBar, ATLAS, CMS, and LHCb are producing and are expected to produce more precise data in the near future [20–26].

The paper is organized as follows: In Section 2, we present the model and further calculate the associated potentials and string tensions in the ultraviolet (UV) and the infrared (IR) regimes. In Section 3, we present the technique for introducing temperature into the model. We divide Section 4 into three subsections where we elaborate on vector potential in Section 4.1, scalar potential energy in Section 4.2, the quark and gluon condensates in Section 4.3, and chiral condensate in Section 4.4. In Section 5, we present our findings and conclusions.

2. The Model

We start with the Lagrangian density:

$$\begin{aligned}\mathscr{L} = &-\frac{1}{4}G(\phi)F_{\mu\nu}F^{\mu\nu} + \frac{1}{2}\partial_\mu\phi\partial^\mu\phi - V(\phi)\\ &-\bar{\psi}\left(i\gamma^\mu\partial_\mu + q\gamma^\mu A_\mu - m_q G(\phi)\right)\psi,\end{aligned} \tag{1}$$

with a potential given as

$$V(\phi) = \frac{1}{2}\left[(\alpha\phi)^2 - 1\right]^2. \tag{2}$$

The Lagrangian together with the potential and tachyon condensation governed by the color dielectric function $G(\phi)$ and dynamics of the scalar field produces the required QCD characteristics.

The equations of motion are

$$\partial_\mu\partial^\mu\phi + \frac{1}{4}\frac{\partial G(\phi)}{\partial\phi}F^{\mu\nu}F_{\mu\nu} + \frac{\partial V(\phi)}{\partial\phi} - \bar{\psi}m_q\psi\frac{\partial G(\phi)}{\partial\phi} = 0, \tag{3}$$

$$-\left(i\gamma^\mu\partial_\mu + q\gamma^\mu A_\mu\right)\psi + m_q G(\phi)\psi = 0, \tag{4}$$

$$\partial_\mu[G(\phi)F^{\mu\nu}] = -\bar{\psi}q\gamma^\nu\psi, \tag{5}$$

where $\mu, \nu = 0, 1, 2, 3$. We are interested in studying static confining potentials that confine the electric flux generated in the model framework, leaving out the magnetic flux which will not be necessary for the current study. With this in mind, we choose magnetic field components $F_{ij} = 0$, such that $F^{\mu\nu}F_{\mu\nu} = -F^{j0}F_{j0} = 2E^2$ and the current density $j^\nu = \bar{\psi}q\gamma^\nu\psi$ restricted to charge density, i.e., $j^\nu = (\rho, \vec{0})$, where $\rho = q/((4/3)\pi R^3)$. Thus, in spherical coordinates, Equation (5) becomes

$$E_r = \frac{\lambda}{r^2 G(\phi)}, \tag{6}$$

where $\lambda = q/4\pi\varepsilon_0$. Expanding Equation (3) in spherical coordinates, we obtain[1]

$$\frac{d^2\phi}{dr^2} + \frac{2}{r}\frac{d\phi}{dr} = \frac{\partial}{\partial\phi}\left[V(\phi) + \frac{\lambda^2}{2}\frac{1}{V(\phi)}\frac{1}{r^4} - \bar{\psi}m_q\psi V(\phi)\right]; \tag{7}$$

we set $G(\phi) = (2\pi\alpha')^2 V(\phi)$ and ignore the term in the order λ^2. Shifting the vacuum of the potential such that $\phi(r) \longrightarrow \phi_0 + \eta$, where $\eta(r)$ is a small perturbation about the vacuum $\phi_0 = 1/\alpha$. We can express Equation (7) as

$$\nabla^2\eta = 4\alpha^2\left(1 - qm_q\delta\left(\vec{r}\right)\right)\eta. \tag{8}$$

We can also determine the bosonic mass from the relation

$$m_\phi^2 = \left.\frac{\partial^2 V}{\partial\phi^2}\right|_{\phi_0} = 4\alpha^2. \tag{9}$$

Also, we define the Dirac delta function such that

$$\delta\left(\vec{r}\right) = \begin{cases}\dfrac{1}{4\pi}\lim\limits_{R\longrightarrow 0}\left(\dfrac{3}{R^3}\right), & \text{if } r \le R,\\ 0, & r > R,\end{cases} \tag{10}$$

where R is the radius of the hadron and r is the interparticle separation distance between the quarks. Now, developing the Laplacian in Equation (8) for particles inside the hadron gives

$$\nabla^2\eta = \left(m_\phi^2 - qm_q^2\right)\eta; \tag{11}$$

here, we have set

$$R = \left(\frac{3m_\phi^2 \left(2\pi\alpha'\right)^2}{4m_q\pi} \right)^{1/3}. \tag{12}$$

A similar expression can be seen in [27, 28], where the mass of the tachyonic mode is determined to be inversely related to the Regge slope, i.e., $M^2 \propto 1/\alpha'$ and $R \propto \sqrt{\alpha'}$. Accordingly, m_ϕ^2 can be identified as the scalar glueball mass obtained from the bound state of gluons (quenched approximation) through the tachyon potential $V(\phi)$. Thus, the tachyonic field ϕ determines the dynamics of the gluons. Expanding Equation (11) leads to

$$\eta'' + \frac{2}{r}\eta' + K\eta = 0, \tag{13}$$

where $K = qm_q^2 - m_\phi^2$. This equation has two separate solutions representing two different regimes, i.e., the infrared (IR) and the ultraviolet (UV) regimes:

$$\begin{aligned} \eta(r) &= \frac{\cosh\left(\sqrt{2|K|}r\right)}{\alpha r\sqrt{2|K|}}, \\ \eta(r) &= \frac{\sin\left(\sqrt{2K}r\right)}{\alpha r\sqrt{2K}}, \end{aligned} \tag{14}$$

for $r \le R$,respectively. We can now determine the confinement potential from the electromagnetic potential

$$V_c(r) = \mp \int E_r dr, \tag{15}$$

where E_r is the electric field modified by the *color dielectric function* $G(r)$. From Equation (6), we can write

$$E_r = \frac{\lambda}{r^2 G(r)}. \tag{16}$$

With the shift in the vacuum, $\phi \longrightarrow \eta + \phi_0$, the tachyon potential and the color dielectric function take the form

$$V(\eta) = G(\eta) = V(\phi)|_{\phi_0} + V'(\phi)\Big|_{\phi_0}\eta + \frac{1}{2}V''(\phi)\Big|_{\phi_0}\eta^2 = \frac{m_\phi^2}{2}\eta^2, \tag{17}$$

and the net confining potential becomes

$$V_c(r, m_q) = -\lambda \frac{\sqrt{\left(m_\phi^2 + m_q^2\right)}\tanh\left[\sqrt{2\left(m_\phi^2 + m_q^2\right)}r\right]}{\sqrt{2}}. \tag{18}$$

Here, we choose the negative part of Equation (15) corresponding to the potential of antiparticle; consequently, we choose $q = -1$ corresponding to an anticolor gluon charge. Besides, confinement in this regime increases with interquark separation r until a certain critical distance $r = r_*$; beyond r_*, hadronization sets in. Since λ depends on the charge q, we can choose $\lambda = -1$. Noting that $\sqrt{2(m_\phi^2 + m_q^2)}r \ll 1$, the string tension can be determined from Equation (18) as

$$\sigma_c(m_q) \simeq m_\phi^2 + m_q^2 \simeq m_L^2, \tag{19}$$

where m_L^2 can be identified as the glueball-meson mixing state obtained from unquenched approximation [29–32]. Now, using $\sigma_c \sim 1$ GeV/fm as adopted in [18, 19] and $m_\phi^2 = 0.99$ GeV^2 corresponding to $m_\phi = 995$ MeV, while $r_* = 1/\sqrt{2\sigma_c}$ [33]. This glueball mass is closer to the scalar glueball mass determined for isoscalar resonance of $f_0(980)$ reported in the PDG as (990 ± 20) MeV [34]. This choice of glueball mass was considered appropriate because we expect m_q to be small but not negative or zero. This choice leads to $m_q = 100$ MeV; this is also within the range of strange (s) quark mass. In the PDG report, $\bar{m}_s = (92.03 \pm 0.88)$ MeV, but much higher values up to 400 MeV are obtained using various fit approaches [35–37], and $\bar{m}_s(1\,\text{GeV}) = (159.50 \pm 8.8)$ MeV are obtained using various sum rules [38, 39]. In this model, the hadronization is expected to start when $r_* = 1/\sqrt{2(m_\phi^2 + m_q^2)} = 0.71$ fm, but for string models such as this, $r \gg r_*$ [33].

On the other hand, the potential in the UV regime becomes

$$V_s(r, m_q) \simeq \left[-\frac{1}{2r} + \frac{\left(m_q^2 - m_\phi^2\right)r}{3} + O\left(r^3\right) \right]. \tag{20}$$

Here, we chose the positive part of the potential, i.e., a potential of a particle, so we set $\lambda = q = 1$. Also, with the string tension

$$\sigma_s = \frac{m_q^2 - m_\phi^2}{3} = \frac{m_s^2}{3}; \tag{21}$$

in both cases, we have set the integration constants $(\tilde{c})$ to zero $(\tilde{c} = 0)$ for simplicity. Assuming that $\sigma_s \sim 1$ GeV/fm as used in [18], we can determine $m_s = 1.73$ GeV, precisely the same as the lightest scalar glueball mass of quantum number $J^{PC} = 0^{++}$ [34, 40–44], and the critical distance is $r_{*s} = 1/\sqrt{\sigma_s}$. The string tension σ is related to the glueball mass by $m(0^{++})/\sqrt{\sigma} = \text{const.}$, where the magnitude of the constant is dependent on the approach adopted for the particular study. In this model framework, we have two different ratios, one in the IR regime and the other in the UV regime, i.e., $m_L/\sqrt{\sigma_c} = 1$ and $m_s/\sqrt{\sigma_s} = 1.73$, respectively. Hence, the ratio is dependent on the regime of interest. The string tension and the dimensionless ratio are precisely

known physical quantities in QCD, because their corrections are known to be the leading order of $O(1/N_c^2)$ in SU(∞) limit. These quantities have been determined by lattice calculations, QCD sum rules, flux tube models, and constituent glue models to be exact [45–47].

From the afore analyses, we can determine $m_q = 2\,\text{GeV}$, while a bound state of quark-antiquark pair would be $m_q^2 = 4\,\text{GeV}^2$. This is compared with the mass of a charm quark $\bar{m}_c(\bar{m}_c) = (1.280 \pm 0.025)\,\text{GeV}$ as reported by PDG [34] and a slightly higher values up to $m_c = 1.49\,\text{GeV}$ in various fits [35–37]. Of cause, the model can take any quark mass greater than one ($m_q > 1$) but less than some critical mass m. Hence, it could be used to successfully study chamonia and bottomonium properties. The only restriction here is that $m_\phi < m_q \leq m$ in the UV regime for the model to work efficiently. In fact, the major results in this section, i.e., the potentials and the string tensions, were reached in [18] and thoroughly discussed at $T = 0$. So, an interested reader can refer to it for step-by-step computations and justifications.

In the model framework, we developed two different potentials, linear confining potential in the IR and a Cornell-like potential in the UV regimes. The potentials obtained from the UV and the IR regimes have confining strengths, m_s^2 and m_L^2, respectively. Linear confining models have been studied by several groups [48–59], and its outcome establishes a good agreement with experimental data for quarkonium spectroscopy together with its decay properties. This potential is motivated by the string model for hadron, where quark and an antiquark pair are seen to be connected by a string that keeps them together. In spite of the successes of this model, it fails to explain the partonic structure of the color particles as observed from deep-inelastic scattering experiments. Consequently, since the QCD theory has generally been accepted as the fundamental theory governing strong interactions, the linear confining model gives a comprehensive description of some sectors of the theory, identified as the IR regime [60, 61]. The Cornell potential, on the other hand, calculated in the UV regime of the model is motivated by lattice QCD (LQCD) calculations [62–72]. Generally, it is represented as

$$V(r) = -\frac{e}{r} + \sigma r, \tag{22}$$

where e and σ are positive constants which are determined through fits. It consists of Coulomb-like part with strength $e = 0.5$ due to single gluon exchange and the linear confining part with strength $\sigma = m_s^2/3$ in the model framework [33, 73, 74]. It is a useful potential in QCD theory because it accounts for the two most important features of the theory, i.e., color confinement and asymptotic free nature of the theory. It reproduces the quarkonium spectrum as well. Also, e and σ can be determined in the framework of heavy quark systems through fitting to experimental data [48–50, 75].

Moreover, the IR model takes in quark masses in the range of 0 to 1 GeV, while the UV model takes in masses greater than $\sqrt{3}$; consequently, there is intermediate mass that can be exploited between 1 and $\sqrt{3}\,\text{GeV}$. This mass range is expected to show hadronization in the IR regime and an asymptotic free behavior in the UV regime without a stable linear confining contribution (QGP). Likewise, the energy suitable for investigating the IR properties is 1.4 GeV and below, deducing from the critical distance r_*, while in the UV regime the maximum energy for confinement is 1 GeV and below judging from the magnitude of r_{*s}, but the process takes place at enormously high energy $r \longrightarrow 0$, where Coulomb potential contribution is dominant. As a result, the model does not account for the behavior of the particles at the intermediate energy regime, apart from knowing that the particles are "asymptotically free" at $r \longrightarrow 0$ and confined at $r \longrightarrow r_{*s}$ and beyond. How the particles behave at the intermediate energy regimes is beyond the scope of this paper. Additionally, perturbative QCD (PQCD) involves hard scattering contribution which requires higher energy and momentum transfer in order to take place. This is referred to as the "asymptotic limit"; thus, the initial and final states of the processes are clearly distinct. Therefore, it has been widely argued that the current energy regime for exploring the QCD theory describes the "subasymptotic" regime, calling for a revision in pure perturbation treatment of the theory. In this case, new mechanisms or models are required to investigate the dynamics of elastic scattering in the *intermediate energy* region [76–80]. One way to investigate this energy region ("soft" behavior) is to use dispersion relation together with operator product expansion (quark-hadron duality) which are collectively referred to as the QCD sum rule [81–83]. Thus, we can study the IR behavior at the lower end of the intermediate energy region while the UV regime lies within the upper end of the intermediate energy region to infinity. The CEBAF (Continuous Electron Beam Accelerator Facility) at Jefferson LAB was initially built to experimentally investigate these intermediate energy regions before it was recently upgraded to cover the high-energy regime.

3. Thermal Fluctuations

In this section, we discuss and propose how temperature can be introduced into the model. Since we have determined in the previous section that the string tension which keeps the quark and antiquark pair in a confined state is dependent on the glueball-meson mixing states m_L and m_s [29, 32], we can determine the confining potentials at a finite temperature if we know exactly how the glueball-meson states fluctuate with temperature. We calculate the temperature fluctuating glueball-meson states directly from Equation (1). Here, we will write the equations in terms of the glueball field η, redefined in dimensionless form such that $\chi = \eta/\phi_0$ for mathematical convenience. The difference between the gluon field and the glueball fields η is that the glueball fields are massive while the gluon fields are not. In this paper, the field ϕ that describes the dynamics of the gluons contains a tachyonic mode; when the tachyons condense, they transform into glueballs η with mass m_ϕ. Accordingly,

$$m_\phi^{*2}\phi_0^2 = -\left\langle \frac{\partial^2 \mathscr{L}}{\partial \chi^2} \right\rangle = \alpha^2\phi_0^2\left(2\pi\alpha'\right)^2\left\langle F^{\mu\nu}F_{\mu\nu}\right\rangle + 4\alpha^2\phi_0^2 - 4m_q\left(\alpha^2\phi_0^2\right)\left(2\pi\alpha'\right)^2\langle\bar{\psi}\psi\rangle \tag{23}$$

[84], where the factor $(2\pi\alpha')^2$ was introduced to absorb the dimensionality of $V(\eta)$ and render $G(\eta)$ dimensionless as explained above. Besides, the theory of gluodynamics is classically invariant under conformal transformation giving rise to vanishing gluon condensation $\langle F_{\mu\nu}F^{\mu\nu}\rangle = 0$ [18, 19]. However, when the scale invariance is broken by introducing quantum correction, say $-|\varepsilon_v|$, the gluon condensate becomes nonvanishing, i.e., $\langle F_{\mu\nu}F^{\mu\nu}\rangle \neq 0$. This phenomenon is referred to as the *QCD energy momentum tensor trace (θ_μ^μ) anomaly* [85]. In this paper, if one disregards the fermions and considers only the gluon dynamics in Equation (1), the potential $V(\phi)$ breaks the scale symmetry and brings about gluon condensation. This phenomenon has been elaborated below in Section 4.3.

To determine the thermal fluctuations, we need to define the field quanta distribution of the mean gauge field $\langle F^{\mu\nu}F_{\mu\nu}\rangle$, $\langle\Delta^2\rangle$ with $\chi = \bar{\chi} + \Delta$ and the spinor fields $\langle\bar{\psi}\psi\rangle$. We find that the fluctuating scalar glueball mass m_ϕ^{*2} does not directly depend on the glueball field χ; hence, no correction to the scalar field will be required. The field quanta distribution of the fields is[2]

$$\left\langle F^{\mu\nu}F_{\mu\nu}\right\rangle = -\frac{\nu}{2\pi^2}\int_0^\infty \frac{p^4 dp}{E_A} n_B(E_A),$$
$$\langle\bar{\psi}\psi\rangle = \frac{\nu_q}{2\pi^2}\int_0^\infty \frac{m_q p^2 dp}{E_\psi} n_F(E_\psi), \tag{24}$$

where $n_B(E_B) = \left(e^{\beta E_A} - 1\right)^{-1}$ is the Bose-Einstein distribution function and $n_F(E_\psi) = \left(1 + e^{\beta E_\psi}\right)^{-1}$ is the Fermi-Dirac distribution function. Also, ν and ν_q are the degeneracies of the gluons and the quarks, respectively, and $\beta = 1/T$. We can now analytically solve these integrals by imposing some few restrictions. We assume a high-energy limit, such that $E \approx p$ for $c = 1 = \hbar$ corresponding to a single particle energy $E^2 = m^{*2} + p^2$; therefore, we find [86, 87]

$$\left\langle F^{\mu\nu}F_{\mu\nu}\right\rangle = -\frac{\nu}{2\pi^2}\int_0^\infty dp\,\frac{p^4}{E_A}\frac{1}{e^{\beta E_A} - 1} = -\frac{T^4\nu}{2\pi^2}\int_0^\infty \frac{x^3 dx}{e^x - 1} = -\frac{\nu\pi T^4}{30} = -\frac{T^4}{T_{cA}^4}\left\langle F^{\mu\nu}F_{\mu\nu}\right\rangle_0, \tag{25}$$

which results in[3]

$$\left\langle F^{\mu\nu}F_{\mu\nu}\right\rangle = \left\langle F^{\mu\nu}F_{\mu\nu}\right\rangle_0\left[1 - \frac{T^4}{T_{cA}^4}\right], \tag{26}$$

and from

$$\langle\bar{\psi}\psi\rangle = \frac{m_q\nu_q}{2\pi^2}\int_0^\infty dp\,\frac{p^2}{E_\psi} n_F(E_\psi) = \frac{\nu_q m_q T^2}{2\pi^2}\int_0^\infty \frac{x dx}{e^x + 1} = \frac{T^2}{4T_{c\psi}^2}\langle\bar{\psi}\psi\rangle_0, \tag{27}$$

we find the quark condensate[4]

$$\langle\bar{\psi}\psi\rangle = -\frac{\langle\bar{\psi}\psi\rangle_0}{4}\left[1 - \frac{T^2}{T_{c\psi}^2}\right]. \tag{28}$$

Here, we used the transformation $x = E/T$ and the critical temperatures

$$T_{cA} = \left(\frac{30\left\langle F^{\mu\nu}F_{\mu\nu}\right\rangle_0}{\nu\pi^2}\right)^{1/4},$$
$$T_{c\psi} = \left(\frac{6\langle\bar{\psi}\psi\rangle_0}{\nu_q m_q}\right)^{1/2}. \tag{29}$$

However, from Equation (23), we can define the dimensionless quantity $\alpha^2\phi_0^2(2\pi\alpha')^2 = \tilde{g}^2$; as a result,

$$m_\phi^{*2}\phi_0^2 = \tilde{g}^2\left\langle F^{\mu\nu}F_{\mu\nu}\right\rangle + 4\alpha^2\phi_0^2 - 4m_q\tilde{g}^2\langle\bar{\psi}\psi\rangle. \tag{30}$$

Now, substituting the thermal averages in Equations (26) and (28) of the fields into the above equation while we absorb the second term derived from the potential into the definition of the first and the third terms at their ground states,

$$m_\phi^{*2}\phi_0^2 = \tilde{g}^2\left\langle F^{\mu\nu}F_{\mu\nu}\right\rangle_0\left[1 - \frac{T^4}{T_{cA}^4}\right] + \tilde{g}^2 m_q\langle\bar{\psi}\psi\rangle_0\left[1 - \frac{T^2}{T_{c\psi}^2}\right]. \tag{31}$$

To proceed, we use the standard definition for determining the QCD vacuum:

$$\theta_\mu^\mu = 4V - \phi\frac{dV}{d\phi}. \tag{32}$$

Using this expression and Equation (2), we obtain

$$\theta_\mu^\mu = 2\left[(\alpha\phi)^4 - 2(\alpha\phi)^2 + 1\right] - \left[2(\alpha\phi)^4 - 2(\alpha\phi)^2\right] = 2 - 2(\alpha\phi)^2; \tag{33}$$

maintaining the term with dependence on ϕ and discarding the constant, the vacuum becomes $B_0 = m_\phi^2\phi_0^2/2$ [84]. Noting that $\left\langle F^{\mu\nu}F_{\mu\nu}\right\rangle_0 = B_0$ represents the vacuum gluon

condensate, we can express

$$m_\phi^{*2} = m_\phi^2\left[1 - \frac{T^4}{T_{cA}^4}\right] + m_q^2\left[1 - \frac{T^2}{T_{c\psi}^2}\right]; \tag{34}$$

here, we set $\tilde{g}^2 = 2$, $\langle F^{\mu\nu}F_{\mu\nu}\rangle_0/\phi_0^2 \approx m_\phi^2/2$ and $\langle\bar{\psi}\psi\rangle_0/\phi_0^2 \approx m_q/2$. The string tension is determined by QCD lattice calculations to reduce sharply with T, vanishing at $T = T_c$ representing melting of hadrons [88–90]. At $T = 0$, we retrieve the result for glueball-meson mixing state m_L^2 in Equation (19), i.e.,

$$m_\phi^{*2}(0) = m_L^2 = m_\phi^2 + m_q^2. \tag{35}$$

We can also retrieve the result in the UV regime m_s^2 if we set $m_\phi^2 \longrightarrow -m_\phi^2$ in Equation (34) at $T = 0$. The nonperturbative feature of QGP is accompanied by a change in the characteristics of the scalar or the isoscalar glueballs and the gluon condensate [91]. This is evident in lattice QCD calculation of pure $SU(3)_c$ theory, pointing to sign changes [86, 87]. Using Equations (17) and (34), the glueball potential can be expressed as

$$\begin{aligned} G(r,T) &= \left(\frac{\cosh\left[\sqrt{2}m_\phi^* r\right]}{m_\phi^* r}\right)^2 \\ &= \left(\frac{\cosh\left[\sqrt{2\left(m_\phi^2\left[1 - T^4/T_{cA}^4\right] + m_q^2\left[1 - T^2/T_{c\psi}^2\right]\right)}\,r\right]}{\sqrt{m_\phi^2\left[1 - T^4/T_{cA}^4\right] + m_q^2\left[1 - T^2/T_{c\psi}^2\right]}\,r}\right)^2. \end{aligned} \tag{36}$$

Accordingly, we can express Equations (18), (19), (20), and (21) in terms of temperature as

$$V_c(r,T,m_q) = \frac{m_\phi^* \tanh\left[\sqrt{2}m_\phi^* r\right]}{\sqrt{2}}, \tag{37}$$

with string tension

$$\sigma_c(m_q,T) = m_\phi^{*2}, \tag{38}$$

$$V_s(r,m_q,T) = -\frac{1}{2r} + \frac{\left(m_q^2\left[1 - T^2/T_{c\psi}^2\right] - m_\phi^2\left[1 - T^4/T_{cA}^4\right]\right)r}{3}, \tag{39}$$

with string tension

$$\sigma_s(m_q,T) = \frac{\left(m_q^2\left[1 - T^2/T_{c\psi}^2\right] - m_\phi^2\left[1 - T^4/T_{cA}^4\right]\right)}{3}. \tag{40}$$

As the temperature is increasing, the confining part shows some saturation near $T \approx T_{c\psi} \approx T_{cA} \approx T_c$ and vanishes completely at $T = T_c$ indicating the commencement of deconfinement and the initiation of the QGP phase. This weakens the interaction of the particles such that the string tension that binds the $\bar{Q}$ and Q reduces and eventually becomes asymptotically free at $T = T_c$. Beyond the critical temperature $T > T_c$, we have the QGP state where the quarks behave freely and in a disorderly manner [92, 93]. The possibility of studying the QGP state in detail with this model exists, but that is beyond the scope of this paper. When we set $\sigma_c(m_q, T) = 0$ and calculate for a common critical temperature by assuming $T_{c\psi} = T_{cA} = 1$ and $m_\phi^2 = \sigma_c - m_q^2$, we will have

$$\begin{aligned} m_\phi^2\left[1 - \frac{T^4}{T_{cA}^4}\right] + m_q^2\left[1 - \frac{T^2}{T_{c\psi}^2}\right] &= 0, \\ \sigma_c - \left(\sigma_c - m_q^2\right)T^4 - m_q^2T^2 &= 0, \end{aligned} \tag{41}$$

where in the last step we substitute $m_\phi^2 = \sigma_c(0) - m_q^2$, and in solving the equation, we bear in mind that $\sigma_c \simeq 1\,\text{GeV/fm}$. Therefore,

$$T_{c1} = \frac{1}{\sqrt{-1 + m_q^2}}; \tag{42}$$

consequently,

$$\sigma_c(T) = m_\phi^2\left[1 - \left(\frac{1}{\sqrt{-1 + m_q^2}}\right)^4\frac{T^4}{T_{c1}^4}\right] + m_\phi^2\left[1 - \left(\frac{1}{\sqrt{-1 + m_q^2}}\right)^2\frac{T^2}{T_{c1}^2}\right]. \tag{43}$$

On the other hand, the common critical temperature in the UV regime can be calculated from

$$\begin{aligned} \frac{m_q^2 - m_\phi^2}{3} - \frac{m_q^2T^2}{3} + \frac{m_\phi^2T^4}{3} &= 0, \\ \sigma_s - \frac{m_q^2T^2}{3} + \frac{\left(m_q^2 - 3\sigma_s(0)\right)T^4}{3} &= 0. \end{aligned} \tag{44}$$

Substituting $\sigma_s \simeq 1\,\text{GeV/fm}$ and solving the equation

$$T_{c2} = \frac{\sqrt{3}}{\sqrt{-3 + m_q^2}}; \tag{45}$$

accordingly,

$$\sigma_s(T) = \frac{m_q^2\left[1 - \left(\sqrt{3}/\sqrt{-3 + m_q^2}\right)^2T^2/T_{c2}^2\right] - m_\phi^2\left[1 - \left(\sqrt{3}/\sqrt{-3 + m_q^2}\right)^4T^4/T_{c2}^4\right]}{3}. \tag{46}$$

It has been found that the bound state of the charm-anticharm state dissolves at $T = 1.1T_c$ [94]. However, the question as to whether heavier quark bound states dissolve at $T = T_c$ [95–97] or temperatures higher than

deconfinement temperature $T > T_c$ [4, 6, 10] still remains open. These two separate pictures have informed different phenomenological models based on confinement and deconfinement transitions to QGP states to explain the observed suppression of J/ψ produced in the RHIC. We present a simple model based on the projection that the $\bar{Q}Q$ bound state melt at $T = T_c$.

4. Vector and Scalar Potentials and Gluon and Chiral Condensates

4.1. Vector Potential. To determine the vector potential, we solve Equation (11) outside the hadron, i.e., $\delta(\vec{r}) = 0$, so

$$\eta'' + \frac{2}{r}\eta' + K_0\eta = 0, \tag{47}$$

where $K_0 = -m_\phi^2$. The solutions of this equation are

$$\begin{aligned} \eta(r) &= \frac{\cosh\left(\sqrt{2|K_0|}r\right)}{\alpha r\sqrt{2|K_0|}}, \\ \eta(r) &= \frac{\sin\left(\sqrt{2K_0}r\right)}{\alpha r\sqrt{2K_0}}, \end{aligned} \tag{48}$$

for IR and UV regimes, respectively; these solutions are equivalent to the solutions in Equation (14) at $m_q = 0$. Now, substituting the solution at the left side of Equation (48) into (16) and into (15), we can determine the vector potential to be

$$V_v(r) = \mp\lambda\frac{m_\phi \tanh\left(\sqrt{2}m_\phi r\right)}{\sqrt{2}}, \tag{49}$$

with string tension

$$\sigma_v \simeq \mp\lambda m_\phi^2. \tag{50}$$

In terms of temperature fluctuations, the potential can be expressed as

$$V_v(T, r) = \mp\lambda\frac{m_{\phi A}^* \tanh\left(\sqrt{2}m_{\phi A}^* r\right)}{\sqrt{2}}, \tag{51}$$

bearing in mind that

$$m_{\phi A}^{*2} = m_\phi^2\left[1 - \frac{T^4}{T_{cA}^4}\right], \tag{52}$$

the corresponding temperature fluctuating string tension [98] becomes

$$\sigma_v(T) \simeq \mp\lambda m_{\phi A}^{*2}. \tag{53}$$

These results can also be derived from Equation (34) for $m_q = 0$.

4.2. Scalar Potential Energy. The scalar potential energy [99–101] for confinement is calculated by comparing Equation (4) with the Dirac equation

$$\left[c\widehat{\alpha}\widehat{p} + \widehat{\beta}m_0c^2 + S(r)\right]\psi = 0, \tag{54}$$

where $\widehat{\alpha}$ and $\widehat{\beta}$ are Dirac matrices and $S(r)$, which is well defined inside and on the surface of the hadron, and zero otherwise is the scalar potential (for detailed explanations, see [18]). Hence, the scalar potential obtained by comparing Equations (4) and (54) can be expressed as

$$\begin{aligned} S(r) &= m_q G(r) = 2\alpha^2 m_q \eta^2 \\ &= \left[\frac{m_q}{\left(m_\phi^2 - qm_q^2\right)r^2}\cosh^2\left(\sqrt{2\left(m_\phi^2 - qm_q^2\right)}r\right)\right]. \end{aligned} \tag{55}$$

For an antiparticle, we set $q = -1$, so we can rewrite the scalar potential in terms of the temperature as

$$S\left(r, m_q, T\right) = \left[\frac{m_q}{m_\phi^{*2}r^2}\cosh^2\left(\sqrt{2}m_\phi^* r\right)\right]. \tag{56}$$

We can now write the net potential energy by adding the vector potential energy and the scalar potential energy; hence,

$$V_{\text{net}}(r) = \mp\frac{q^2 m_\phi \tanh\left(\sqrt{2}m_\phi r\right)}{4\sqrt{2}\pi} + \left[\frac{m_q}{m_\phi^2 r^2}\cosh^2\left(\sqrt{2}m_\phi^*(0)r\right)\right] \tag{57}$$

[102, 103], and in terms of temperature, we can express

$$\begin{aligned} V_{\text{net}}\left(r, m_q, T\right) = \mp&\frac{q^2 m_{\phi A}^* \tanh\left(\sqrt{2}m_{\phi A}^* r\right)}{4\sqrt{2}\pi} \\ &+ \left[\frac{m_q}{m_\phi^{*2}r^2}\cosh^2\left(\sqrt{2}m_\phi^* r\right)\right]. \end{aligned} \tag{58}$$

4.3. Gluon Condensates. We calculate the energy momentum tensor trace, θ_μ^μ, from the relation

$$\theta_\mu^\mu = 4V(\eta) + \eta\Box\eta. \tag{59}$$

Substituting the equation of motion Equation (3) into the above equation yields

$$\theta_\mu^\mu = 4V(\eta) - \eta\frac{\partial V}{\partial \eta} - \frac{\eta}{4}\frac{\partial G}{\partial \eta}F^{\mu\nu}F_{\mu\nu} + q\delta\left(\vec{r}\right)m_q\eta\frac{\partial G}{\partial \eta} = 4\tilde{V} + \tilde{G}F^{\mu\nu}F_{\mu\nu} - 4q\delta\left(\vec{r}\right)m_q\tilde{G} = 4\tilde{V}_{\text{eff}} + \tilde{G}F_{\mu\nu}F^{\mu\nu}, \tag{60}$$

where

$$\tilde{V} = V - \frac{\eta}{4}\frac{\partial V}{\partial \eta}, \quad \tilde{G} = -\frac{\eta}{4}\frac{\partial G}{\partial \eta}, \quad \tilde{V}_{\text{eff}} = \tilde{V} - q\delta\left(\vec{r}\right)m_q\tilde{G}. \tag{61}$$

Moreover, the energy momentum tensor trace θ_μ^μ for the classical QCD chiral effective Lagrangian [93, 104] is given as

$$\theta_\mu^\mu = \sum_f m_f q_f \bar{q}_f - \frac{b\alpha_s}{8\pi}F^{a\mu\nu}F^a_{\mu\nu}, \tag{62}$$

where $\beta(g) = -b\alpha_s/(4\pi)$ ($b = 11$ depicts pure gluodynamics) is the QCD β-function, m_f is the current quark mass matrix, and q_f is the quark field. Simplifying $\tilde{V}_{\text{eff}}$ in Equation (60), we find

$$\tilde{V}_{\text{eff}}(\eta) = \frac{1}{4}m_\phi^2\eta^2 - qm_q\delta(r)\left(-\frac{m_\phi^2}{4}\eta^2\right) = \frac{1}{4}m_L^2\eta^2, \text{for } q = 1, \tag{63}$$

so

$$\theta_\mu^\mu = \frac{1}{4}m_L^2\eta^2 - \frac{G(\eta)}{2}F_{\mu\nu}F^{\mu\nu}, \text{where } G(\eta) = V(\eta) = \frac{m_\phi^2\eta^2}{2}. \tag{64}$$

Accordingly, comparing this with (62), we can identify $\sum_f m_f = m_L^2$ (glueball-meson mixing mass), $\sum_f q_f\bar{q}_f = \eta^2$ (glueball field), and $b\alpha_s/(4\pi) = G(\eta) = -\beta(1/r^2)$ QCD β-function. To determine the strong running coupling, we note that $G(\eta) = \eta G'(\eta)/2$, so using the renormalization group theory [105]

$$\beta\left(Q^2\right) = Q^2\frac{d\alpha_s\left(Q^2\right)}{dQ^2}, \tag{65}$$

we can deduce

$$\beta\left(\frac{1}{r^2}\right) = -\eta\frac{d}{d\eta}\left(\frac{1}{2}G(\eta)\right); \tag{66}$$

consequently, the strong running coupling becomes $\alpha_s(1/r^2) = G(\eta)/2$, where we can relate $Q \longrightarrow 1/r$. Using the solution at the right side of Equation (14), we can express

$$\alpha_s\left(\frac{1}{r^2}\right) = \left[1 - \frac{2Kr^2}{3}\right] = \left[1 + \frac{2\left(m_\phi^2 + m_q^2\right)r^2}{3}\right], \text{for } q = -1 \longrightarrow \alpha_s\left(q^2\right) = \left[1 - \frac{2}{3}\frac{m_L^2}{q^2}\right]. \tag{67}$$

Noting that $Q^2 \equiv -q^2$, where Q^2 is the space-like momentum and q^2 is the four-vector momentum. To eliminate the Landau ghost pole that occurs at $q^2 \longrightarrow 0$, we assume that there is dynamically generated "gluon mass" at $q^2 \longrightarrow 0$, i.e., $q^2 \cong m_A^2$ [106, 107]. Now, relating the results in Equation (60) with the standard vacuum expectation value of QCD energy momentum tensor trace,

$$\left\langle\theta_\mu^\mu\right\rangle = -4|\varepsilon_v| \tag{68}$$

[18, 19], we can write

$$\left\langle\tilde{G}(\phi)F^{\mu\nu}F_{\mu\nu}\right\rangle = -4\left\langle|\varepsilon_v| + \tilde{V}_{\text{eff}}(\eta)\right\rangle. \tag{69}$$

Now, we rescale $\tilde{V}_{\text{eff}}$ with the QCD vacuum energy density $-|\varepsilon_v|$ such that $\tilde{V}_{\text{eff}} \longrightarrow -|\varepsilon_v|\tilde{V}_{\text{eff}}$, and using the potential of the glueball fields defined in Equation (17), we obtain

$$\left\langle\frac{m_\phi^2\eta^2}{4}F^{\mu\nu}F_{\mu\nu}\right\rangle = 4|\varepsilon_v|\left\langle 1 - \frac{m_L^2\eta^2}{4}\right\rangle; \tag{70}$$

here, we used $\tilde{V}_{\text{eff}} = 1/4(m_\phi^2 + qm_q^2)\eta^2 = (m_L^2/4)\eta^2$ for $q = 1$. Also, at the classical limit $\varepsilon_v \longrightarrow 0$, we have vanishing gluon condensate $\langle F_{\mu\nu}F^{\mu\nu}\rangle = 0$. The vacuum expectation value (VEV) of the gluon condensate was determined in [108–110] using Yang Mills theory with an auxiliary field ϕ, where the fluctuations around ϕ give rise to the glueball mass, $m(0^{++})$. It was observed that in the nonvanishing VEV, the gluon acquire a common mass, m_A, and the ratio $m(0^{++})/m_A$ in the leading order is

$$\frac{m(0^{++})}{m_A} \cong \sqrt{6}. \tag{71}$$

The nonvanishing condensate was attributed to the pair condensate of transverse gluons. Juxtaposing that to the results in Equation (70), we can identify

$$m_A^2 = \frac{m_L^2}{4}. \tag{72}$$

Other calculations based on QCD theory [111] also show that the nonvanishing gluon condensate in the

absence of fermions can be expressed in terms of the gluon mass as

$$m_g^2 = \left(\frac{34N\pi^2}{9\left(N^2-1\right)}\left\langle\frac{\alpha_s}{\pi}G^{\mu\nu}G_{\mu\nu}\right\rangle\right)^{1/2}, \tag{73}$$

where N is the number of colors and α_s is the strong coupling constant. This relation also show a proportionality between gluon mass and the nonvanishing condensate—more discussions relating to this subject can also be found in [112, 113]. Again, from the left side of Equation (70), we can deduce the expression $\langle(G(\eta)/2)F^{\mu\nu}F_{\mu\nu}\rangle = \langle\alpha_s(1/r^2)F^{\mu\nu}F_{\mu\nu}\rangle$; hence, the expression in the angle brackets at the right side of Equation (70) is equivalent to Equation (67). Following the discussions at the latter part of Section 2, $m_L = 1\,\text{GeV}$ so we can determine the gluon mass as $m_A = 500\,\text{MeV}$. This can be compared to the result determined from QCD lattice simulation, projecting the gluon mass to be $m_A = 600 \sim 700$ MeV [114–116]. Some heavier gluon masses have also been determined closed to ~ 1 GeV using phenomenological analysis [117, 118] and some QCD lattice studies [119]. Quark and gluon condensates are responsible for confinement, glueball formation, and hadron mass formation [80, 104, 120, 121]. The QCD vacuum at the ground state enables us to study the characteristics of the QGP, dynamics of phase transitions, and hadronization. All these properties are a result of the nonperturbative nature of QCD theory in some regimes (IR) and cannot be studied using the usual perturbative QCD theory.

To determine the temperature fluctuations in the gluon mass m_A and the gluon condensate, we need to correct the temperature in the glueball field χ. The gluon mass is formed due to screening of the gluons in the vacuum or at a temperature where the constituent quarks dissolve into gluons [122]. The temperature can be introduced by defining the glueball field such that $\chi = \bar{\chi} + \Delta$, so $\eta = \phi_0(\bar{\chi} + \Delta)$, with the restriction $\langle\Delta\rangle = 0$ to avoid the occurrence of cross-terms in the thermal average. Again, $\bar{\chi}$ represents the mean glueball field, and the angle brackets represent the thermal average. We express the fluctuation $\langle\Delta^2\rangle$ in terms of field quanta distribution as defined for the gauge and the fermion fields in Equations (26) and (27), respectively, i.e.,

$$\left\langle\Delta^2\right\rangle = \frac{1}{2\phi_0^2\pi^2}\int_0^\infty dk\frac{k^2}{E_\eta}\frac{1}{e^{\beta E_\eta}-1} = \frac{T^2}{2\phi_0^2\pi^2}\int_0^\infty\frac{xdx}{e^x-1} = \frac{T^2}{12\phi_0^2}. \tag{74}$$

Reverting to Equation (3) and the definition $\eta = \phi_0(\bar{\chi} + \Delta)$, we can determine the thermal average directly from the equation of motion to be

$$\begin{aligned}\left\langle\frac{1}{4}\frac{\partial G}{\partial\eta}F^{\mu\nu}F_{\mu\nu}\right\rangle &= \left\langle\frac{\partial V(\eta)}{\partial\eta}\left(qm_q\delta(r)-1\right)\right\rangle,\\ \left\langle\frac{m_\phi^2\eta}{4}F^{\mu\nu}F_{\mu\nu}\right\rangle &= -\left\langle\left(m_\phi^2 - qm_q^2\right)\eta\right\rangle;\end{aligned} \tag{75}$$

clearly, $\bar{\eta} = \bar{\chi} = 0$ is a solution; hence, $\langle\eta^2\rangle = \phi_0^2\langle\Delta^2\rangle$.

Moreover, substituting Equation (74) for temperature fluctuations in η^2 into Equation (70), the gluon condensate becomes

$$\begin{aligned}\left\langle\frac{m_\phi^2\eta^2}{4}F^{\mu\nu}F_{\mu\nu}\right\rangle &= 4|\varepsilon_v|\left[1-\frac{m_L^2\phi_0^2}{4}\left(\frac{T^2}{12\phi_0^2}\right)\right]\\ &= 4|\varepsilon_v|\left[1-\frac{T^2}{T_{c\eta}^2}\right], \text{ where } T_{c\eta}^2 = \frac{48}{m_L^2}.\end{aligned} \tag{76}$$

The QCD vacuum at an extremely high temperature and density has an important significance in both elementary particle physics and cosmology. In cosmology, it can be used to explain the evolution of the universe at extremely higher temperatures when matter becomes super dense and hadrons dissolve into a "soup" of their constituents—quarks and gluons. At such superdense matter regimes, the quarks become very close and asymptotically free, so the quarks are no longer confined into hadrons. It is important to note that the energy density is related to temperature as $\rho \propto T^4$, so the density increases with temperature. This phase of matter was proposed [123, 124] after the asymptotic free [125, 126] nature of the QCD theory [127] was determined. Currently, almost all the accepted models for the cooling of the universe are based on phase transitions, either first or second order of spontaneous symmetry breaking of fundamental interactions [128–130]. On the other hand, the standard model (SM) of elementary particle physics suggests two of such phase transitions [130]. It shows an electroweak symmetry (EW) breaking at temperatures in the order of $T \sim 100\,\text{GeV}$ which generates mass to elementary particles such as quarks. It is also associated with the observed baryon-number-violation of the universe [131]. This transition is determined to be an analytical crossover in lattice simulations [132].

Again, spontaneous chiral symmetry breaking is next; it is known to occur at temperatures in the order of $T \sim 200$ GeV. Nevertheless, we have hadronic matter below this temperature, and above it, we have an expected transit into the QGP phase. This phase is also important in understanding the evolution of the early universe. Some references on this subject using nonperturbative lattice QCD models can be found in [133, 134]. Particularly, knowing that the baryon chemical potential μ_B is expected to be smaller than the usual hadron mass, $\mu_B \approx 45\,\text{MeV}$ at $\sqrt{s_{NN}} = 200\,\text{GeV}$ [135], and almost vanishing $\mu_B \approx 0\,\text{GeV}$ in the early universe. It is suitable to model inflation of the early universe at high temperatures and low baryon densities. There is strong evidence that confinement of quarks into hadrons is a low-energy phenomenon [133, 136, 137], but it strongly suggests that QCD phase transition is a crossover. Numerically, it has been established that at $\mu_B = 0\,\text{GeV}$, the two-phase transitions possibly coincide, i.e., deconfinement and chiral symmetry restoration rendering the chiral effective theory invalid [138]. From our model framework, Equation (76), we obtain confinement at $T < T_c$, deconfinement and restoration of chiral symmetry at $T = T_c$, and QGP phase at $T > T_c$.

Deducing from Equation (76), the thermal fluctuating gluon mass becomes

$$m_A^{*2} = \left(\frac{m_L^2}{48\phi_0^2}\right)T^2 = g^2T^2, \tag{77}$$

where $g^2 = m_L^2/48\phi_0^2$ is a dimensionless coupling constant [122, 139]. This results look similar to the Debye mass obtained from the leading order of QCD coupling expansion at higher temperatures and zero chemical potential, $m_D = gT$ [140]. This mass is obtained from the lowest order perturbation QCD theory [141], but it is known to be resulting from the IR behavior of the theory [142]. This mass occurs at temperatures greater than the deconfinement temperature T_c due to the melting of $\bar{Q}Q$ bound states [11, 140]; generally, it is referred to as *Debye screening mass of color charges*.

Furthermore, the experimental evidence of QCD vacuum condensates dates back from the pre-QCD era 1950-1973 to post-QCD after 1974, and it still remains an issue of interest. The QCD vacuum condensate informs color confinement and chiral symmetry breaking which are fundamentals of strong interactions. The condensate is a very dense nonperturbative state of matter consisting nonvanishing gluon and quark condensates, in theories containing effective quarks, interacting in a haphazard manner [80]. Since quarks and gluons are not observed directly in nature, these characteristics are difficult to observe experimentally; only colorless (baryons) or color neutral (mesons) hadrons are observed. However, much is known about the QCD vacuum, credit to the fast-evolving QCD sum rule which explores the gauge invariant formalism to explain the nonperturbative nature of the condensates [143, 144]. That notwithstanding, the QCD sum rule gives good results at the intermediate energy region and poses some short falls at large distance regimes where color confinement and chiral symmetry breaking are more pronounced. So, a resort is made to the Vacuum Correlator Method (VCM) to give a comprehensive description of all the possible QCD phenomena involved ([145–148]. The VCM is based on gauge invariant Green's function of colorless or color neutral objects expressed in path integral formalism using field correlators instead of propagators.

4.4. Chiral Condensate. *Chiral symmetry breaking* is one of the known physical properties of the nonperturbation regime of QCD theory besides the famous *color confinement*. Mass splitting of the chiral partner observed in the hadron spectrum and *Goldstone bosons* ($\pi^{\pm}$ and π^0) which appear due to spontaneous symmetry breaking leading to *color confinement* are strong evidence of chiral symmetry breaking [149–151] in QCD vacuum [152]. The presence of quark mass breaks the chiral symmetry explicitly. With these background and other theoretical considerations, it is believed that there is chiral condensate in the vacuum which is proportional to the expectation value of the fermionic operator or the quark condensate $\langle\bar{\psi}\psi\rangle$. However, increasing temperature augments the thermal excitations of the hadrons due to an increase in the density ($\rho \propto T^4$) of their quark constituents. This decreases the vacuum condensate until it eventually vanishes at a critical temperature T_{cq} resulting into restoration of the chiral symmetry. At this temperature, the hadrons undergo phase transition to deconfinement and quark-gluon plasma (QGP) phase. Increasing baryon density has the same consequences on the QGP phase and chiral condensate similar to temperature increase [153, 154]. To begin the calculation of the *chiral condensate*, one needs to take into account the dependence of the hadron masses on the current quark mass m_q. Some known first principle approaches to this subject that give a consistent account of hadrons and their quark mass dependent are *Chiral Perturbation Theory* (ChPT) [155], lattice QCD (lQCD) [156], and *Dyson-Schwinger Equation* (DSE) [157, 158].

However, the dominant degrees of freedom for QCD at low energies are hadrons [159, 160]. Particularly, pions and kaons interact weakly according to Goldstone theory; hence, they can be treated as free particles. Consequently, the standard relation for calculating the chiral condensate, $\langle\bar{q}q\rangle$, can be derived from Equation (1) as

$$\langle\bar{q}q\rangle = -\left\langle\frac{\partial\mathscr{L}}{\partial m_q}\right\rangle \tag{78}$$

[155], where $\langle\bar{q}q\rangle$ is significant for *spontaneous chiral symmetry breaking* (SχSB) and the angle brackets represent thermal average. Subtracting the fundamental vacuum condensate $\langle\bar{q}q\rangle_0$ to ensure that the condensate has its maximum $T = 0$ [161], we can express the above relation as

$$\langle\bar{q}q\rangle = \langle\bar{q}q\rangle_0 - \left\langle\frac{\partial\mathscr{L}}{\partial m_q}\right\rangle; \tag{79}$$

here, details of the vacuum condensate $\langle\bar{q}q\rangle_0$ [162, 163] are of no importance to the analyses. All the information needed to study the contributions of the hadrons is contained in the medium dependent term. From Equation (1) and using the expression in Equation (17) derived from $\phi(r) \longrightarrow \phi_0 + \eta$, we obtain

$$\left\langle\frac{\partial\mathscr{L}}{\partial m_q}\right\rangle = \langle G(\eta)\bar{\psi}\psi\rangle = \left\langle\frac{m_\phi^2\eta^2}{2}\bar{\psi}\psi\right\rangle. \tag{80}$$

Thus, the chiral condensate is proportional to the glueball potential $G(\eta)$ which has its maximum condensate at $G(\eta) \longrightarrow 0$ [18, 19]. The quark density $\langle\bar{\psi}\psi\rangle$ is a measure of the strength of the condensate and SχSB. At $\langle\bar{\psi}\psi\rangle = 0$, we have an exact chiral symmetry, deconfinement, and QGP phase, while nonvanishing quark condensate, $\langle\bar{\psi}\psi\rangle \neq 0$, is the regime with S$\chi$SB and *color confinement* [164, 165]. Therefore, $\langle\bar{\psi}\psi\rangle$ serves as an order parameter that determines the phase transitions. Since the explicit pion degrees of freedom is significant for studying chiral symmetry restoration at low temperature and quark densities, $\langle\bar{\psi}\psi\rangle$ is constituted with *up* (u) and *down* (d) quarks. Eventually, protons and neutrons are also composed of

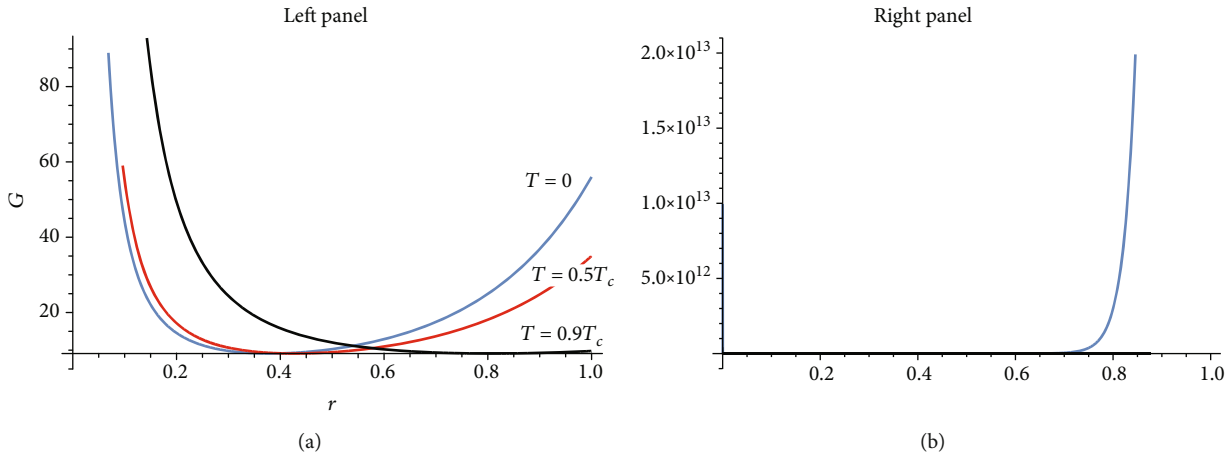

FIGURE 1: A graph of glueball potential $G(r, T)$, against r, T for $m_q = 0.1$ (a) and $m_q \longrightarrow \infty$ (b).

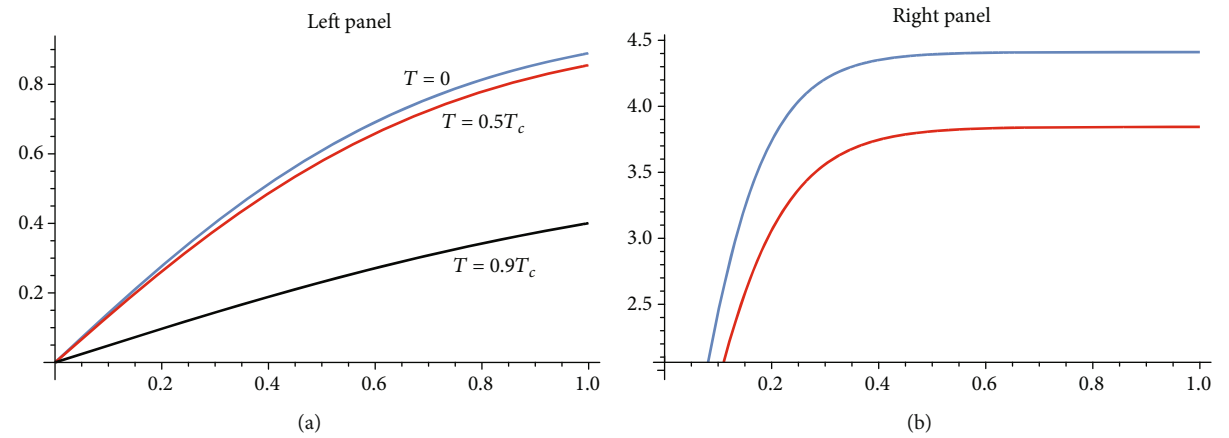

FIGURE 2: A graph of net confining potential, $V_c(r, T)$, against r, T for $m_q = 0.1$ (a) and $m_q \longrightarrow \infty$ (b).

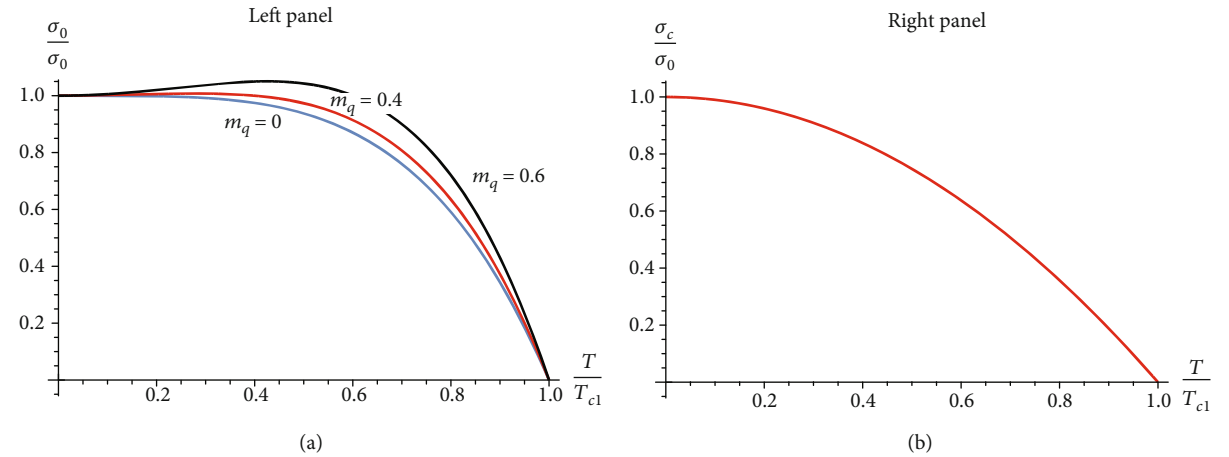

FIGURE 3: A graph of string tension, $\sigma_c(T)/\sigma_0$, against T/T_{c1} for different values of m_q (a) and $m_q \longrightarrow \infty$ (b).

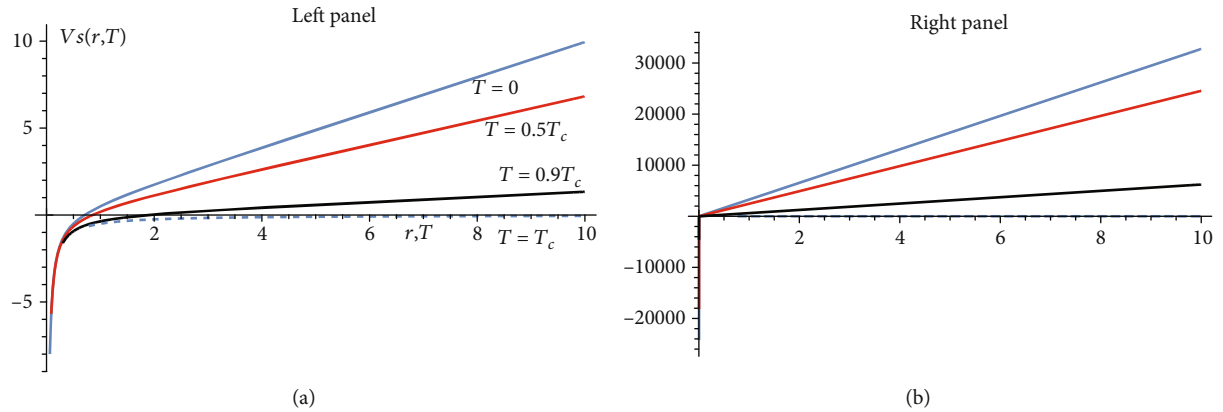

Figure 4: A graph of net potential in the UV regime, $V_s(r, T)$, against (r, T) for $m_q = 2$ (a) and $m_q \longrightarrow \infty$ (b).

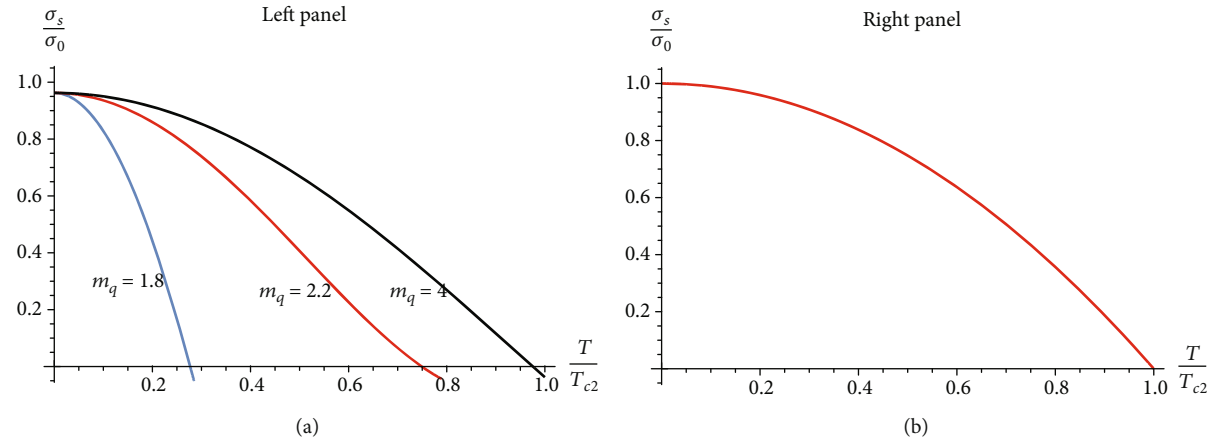

Figure 5: A graph of string tension, $\sigma_s(T)/\sigma_0$, in the UV regime against T/T_{c2} for different values of m_q (a) and $m_q \longrightarrow \infty$ (b).

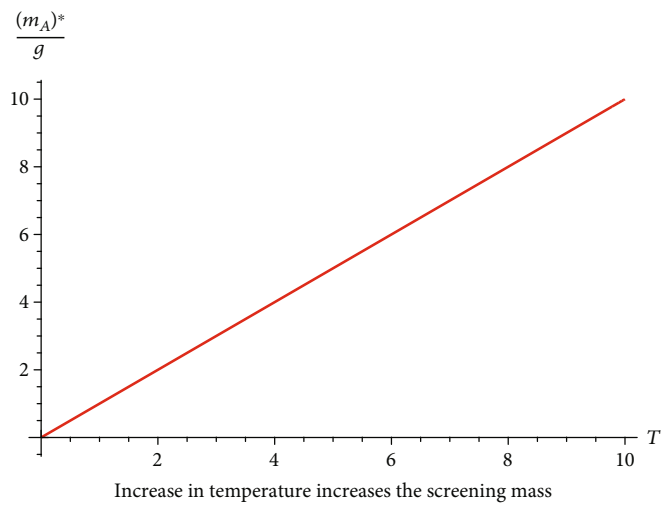

Figure 6: A graph of fluctuating gluon mass m_A^*/g with temperature T.

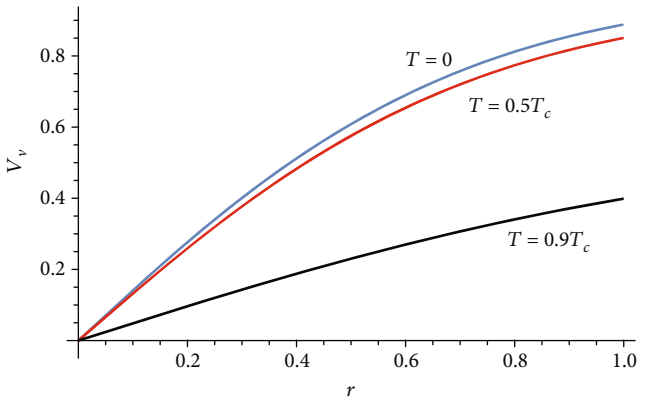

Figure 7: A graph of vector potential $V_v(T, r)$ against T, r for specific values of T.

similar quark constituents; hence, in QCD with two flavor constituents,

$$\langle \bar{\psi}\psi \rangle = \langle \bar{q}_i q_i \rangle = \langle \bar{u}u \rangle + \langle \bar{d}d \rangle. \tag{81}$$

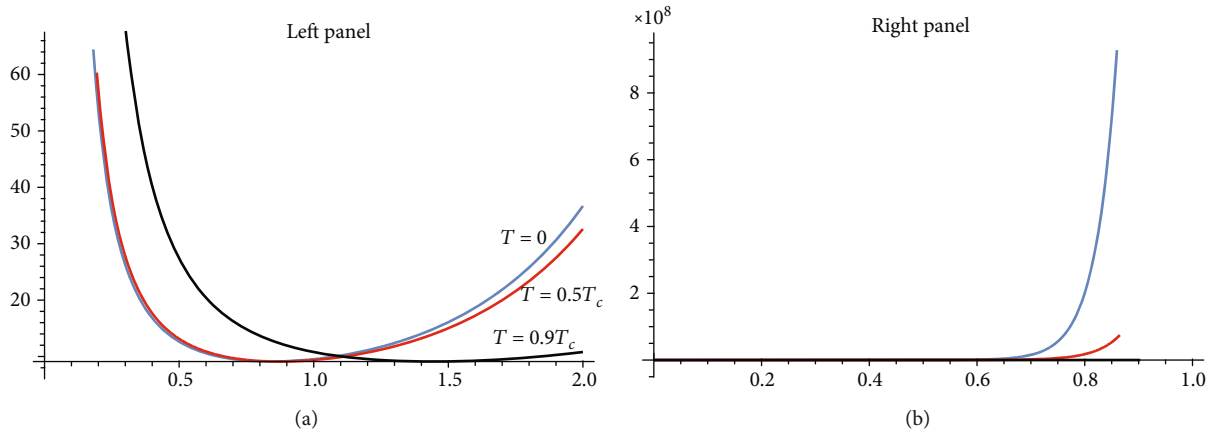

FIGURE 8: A graph of scalar potential energy, $S(r, T)$, against r, T for $m_q = 0.1$ (a) and $m_q \longrightarrow \infty$ (b).

Additionally, in terms of temperature

$$\begin{aligned}\langle\bar{q}q\rangle &= \langle\bar{q}q\rangle_0 - \left[\frac{m_\phi^2}{2}\left(\frac{T^2}{12}\right)\left(\frac{m_q \nu_q T^2}{24}\right)\right] \\ &= \langle\bar{q}q\rangle_0 - \left[\frac{m_\phi^2 m_q \nu_q}{576}T^4\right] = \langle\bar{q}q\rangle_0\left[1 - \frac{T^4}{T_{cq}^4}\right],\end{aligned} \tag{82}$$

where in the first step, we used the results in Equations (27) and (74), bearing in mind that $\langle\eta^2\rangle \simeq \phi_0^2\langle\Delta^2\rangle$ and

$$T_{cq} = \left(\frac{576}{m_\phi^2 m_q \nu_q}\langle\bar{q}q\rangle_0\right)^{1/4}. \tag{83}$$

Thus, at $T = T_{cq}$, the chiral symmetry gets restored in the model framework. If one intends to investigate the behavior of the chiral condensation with varying quark mass m_q, we can define the critical temperature as

$$T_{cq} = \left(\frac{576}{m_\phi^2 \nu_q}\langle\bar{q}q\rangle_0\right)^{1/4}, \tag{84}$$

corresponding to a condensate

$$\langle\bar{q}q\rangle = \langle\bar{q}q\rangle_0\left[1 - m_q\frac{T^4}{T_{cq}^4}\right]. \tag{85}$$

Also, an evidence from lQCD confirms that at the confinement phase the chiral symmetry is spontaneously broken down [165, 166] to the flavor group, i.e.,

$$\mathrm{SU}(2)_R \times \mathrm{SU}(2)_L \longrightarrow \mathrm{SU}(2)_V, \tag{86}$$

with associated three Goldstone bosons ($\pi^\pm$ and π^0) which spontaneously break the chiral symmetry. For three quark flavors, we have

$$\mathrm{SU}(3)_R \times \mathrm{SU}(3)_L \longrightarrow \mathrm{SU}(3)_V; \tag{87}$$

here, there are eight Goldstone bosons ($\pi^\pm, \pi^0, K^\pm, K^0, \bar{K}^0$, and η) involved (see References [167, 168]).

Again, a highly excited state in high-energy hadronic collisions leads to the formation of disoriented chiral condensate which can later decay into ordinary vacuum through coherent emission of low momentum pions. This process is theoretically synonymous to the Higgs mechanism that leads to the release of Goldstone bosons. This leaves a signature of color confinement eventually [169]. Even though the idea of chiral condensate was speculative at its inception in the 1990's [170–174], it has attracted several theoretical and experimental attention subsequently. Besides its simplicity, it is also motivated by the discovery of the "so-called" Centauro events in cosmic ray [175–177] where clusters consisting charged and neutral pions were observed. The chiral condensate has also been studied theoretically in the light of high-energy heavy ion collisions [178, 179] due to the high energies involved at the collision zone; a hot chirally symmetric state (QGP) is formed in the process. Because of the fast expanding nature of the system at the early stages, it is quenched down to a low temperature where chiral symmetry is spontaneously broken down. Several experiments have since been set up to investigate this phenomena, keys among them are the cosmic ray experiment [175, 176], nucleon-nucleon collisions at CERN [180–182], Fermi LAB [183], particularly, MiniMAX experiment [184], nucleon-nucleon collisions at CERN SPS ([185–188], and the RHIC [189, 190]. It also forms part of the heavy ion collision programme carried out with the multipurpose detector ALICE, at LHC [191, 192].

5. Conclusion

Following the discussions in [18] for the constituent quark masses, we can deduce that the constituent quark masses of this model are $M(r \longrightarrow r_*) = 2m_q = 200\,\mathrm{MeV}$ and $M(r \longrightarrow 0) = 2m_q = 4\,\mathrm{GeV}$ for the IR and the UV regimes, respectively. Thus, the potential in the IR and the UV regimes can take masses within the ranges $0 \le m_q \le 200\,\mathrm{MeV}$ and $2 \le m_q \le 4\,\mathrm{GeV}$, respectively. Hadronization is expected to set in, in the IR and the UV regimes for $m_q > 200$ and $m_q > 4$, respectively, since we have adopted the lattice simulation

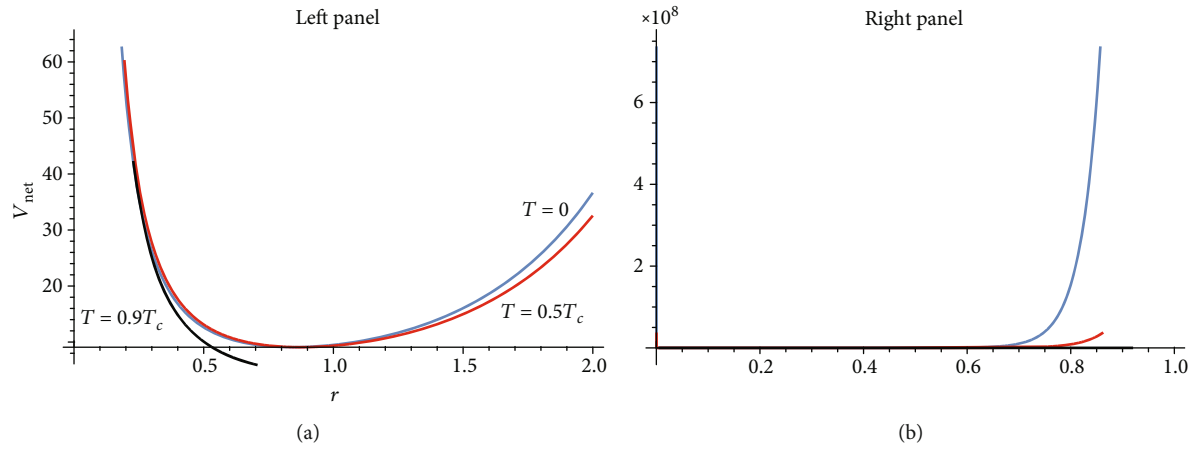

FIGURE 9: A graph of net potential energy, $V_{net}(r, T)$, against r, T for $m_q = 0.1$ and an infinite m_q.

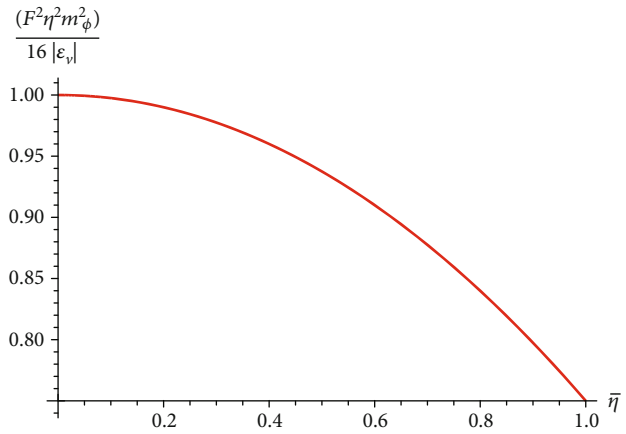

FIGURE 10: A graph of gluon condensate $\langle (m_\phi^2 \eta^2) F^{\mu\nu} F_{\mu\nu} \rangle / (16 \mid \varepsilon_v \mid)$ against $\bar{\eta}$.

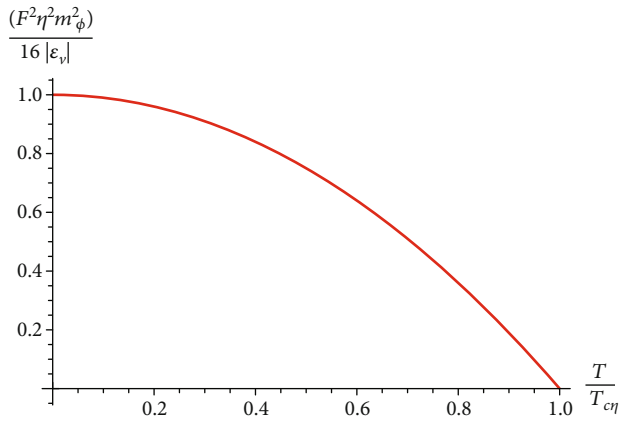

FIGURE 11: A graph of gluon condensate $\langle (m_\phi^2 \eta^2) F^{\mu\nu} F_{\mu\nu} \rangle / (16 \mid \varepsilon_v \mid)$ against $T/T_{c\eta}$.

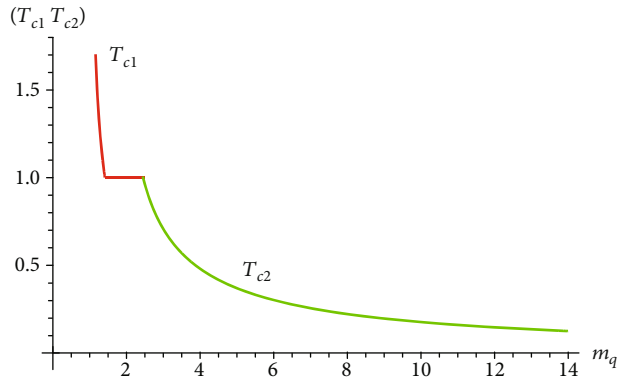

FIGURE 12: A phase diagram for T_{c1} and T_{c2} against quark mass m_q.

results for the string tension $\sigma \sim 1$ GeV/fm, and noticing that $\sigma = 1/(2\pi\alpha')$ as shown in many confining string models [28, 193]. The choice $(2\pi\alpha')^2 = 1$ used throughout the paper is in order. In the framework of the model, the glueball field χ does not contribute to the fluctuations in the scalar glueball mass m_ϕ^{*2}, while the only candidate that contributes to the fluctuating gluon mass m_A^{*2} is the glueball field. On the other hand, the gauge fields, the spinor fields, and the glueball fields all contribute to the gluon condensate $\langle (m_\phi^2 \eta^2/4) F^{\mu\nu} F_{\mu\nu} \rangle$ and chiral condensate. Thus, the condensates are important in understanding QCD theory but difficult to study experimentally due to the haphazard nature of interactions among these fields in the vacuum. Also, ν_q and ν are the degeneracies of quarks and gluons, and they take in the values, 6 and 16 for SU(2) and SU(3) representations, respectively. These degeneracies are important in determining the critical temperatures of the model. The critical temperatures are small when the degeneracies are infinitely large, and when there is no degeneracies at all ($\nu, \nu_q \longrightarrow 0$), the critical temperature becomes infinitely large; same is true for quarks and gluons as presented in Equations (29) and (86).

The model produces two forms of temperature corrections to the string tension, $-T^2$ coming from the spinors (quarks) and $-T^4$ from the gauge fields (gluons). The $-T^2$ correction to the string tension has been corroborated by some QCD lattice calculations [89, 194, 195] and some phenomenological models [19]. That notwithstanding, $-T^4$

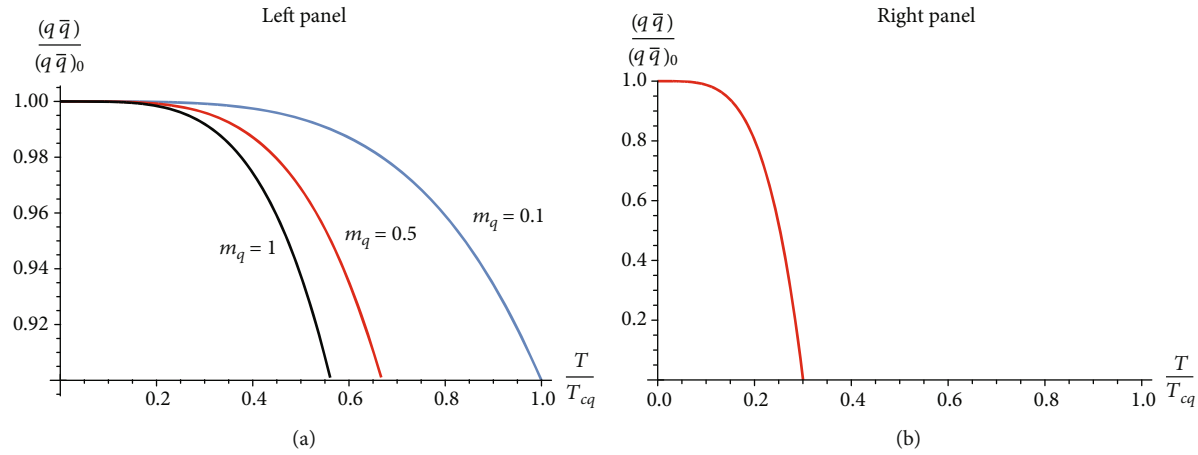

FIGURE 13: A graph of chiral condensate against T/T_{cq} for different values of m_q (a) and $m_q \longrightarrow \infty$ (b).

correction to the string tension has also been proposed by some phenomenological models [28]. Both corrections give the correct behavior of the string tension, i.e., it should reduce sharply with temperature and break or vanish at $T = T_c$for simple models such as the one discussed here. For simplicity, we used $T_{cA} = T_{c\psi}$ for some of the analyses—particularly, the potentials—but there is no evidence that these two critical temperatures have the same magnitude. In any case, such assumption is informed and does not affect the results or the analyses. However, there is a discussion in [196] suggesting that $T_{c\psi} > T_{cA}$ ($T_{c\psi} \sim 270$ MeV and $T_{cA} \sim 170$ MeV) or at least a discrepancy of about 3% reported in [197]. Using the magnitude of the string tension and the scalar glueball mass m_ϕ calculated above, we obtained two different glueball-meson states corresponding to $m_L = 1$ GeV and $m_s = 1.73$ GeVfor the IR and UV regimes, respectively. The gluon mass was also determined as $m_A = 500$ MeV. The critical distance for confinement in the IR regime has been determined to be $r_* = 0.71$ fm, and its corresponding value in the UV regime is $r_{*s} = 1/\sqrt{\sigma_s} = 1$ fm. Similarly, r_* and r_{*s} can be expressed as a function of temperature like the string tensions.

Some of the major results obtained are displayed on a graph to make it easy to see their behavior. Since we have extensively studied and discussed the corresponding results for $T = 0$ in [18], we will concentrate on the results with temperature fluctuations. We plot the glueball potential Equation (36) and its behavior with temperature in Figure 1. The confining potential Equation (37) in the IR regime for finite and infinite m_q is plotted in Figure 2 and its string tension Equation (38) plotted in Figure 3. The potential in the UV regime Equation (39) is plotted in Figure 4 displaying how Cornell-like potential obtained varies with temperature for finite and infinite quark mass limits and their string tension in Equation (40) displayed in Figure 5. The gluon mass Equation (77) which possesses all the characteristics of Debye mass is displayed in Figure 6. The vector potential Equation (51) which represents *chromoelectric flux* confinement is displayed in Figure 7. The scalar potential energy Equation (55) and the corresponding net potential energy Equation (58) for finite and infinite m_q are plotted in Figures 8 and 9, respectively. The gluon condensates calculated in Equations (70) and (76) are also displayed in Figures 10 and 11, respectively. The color dielectric function in Equation (17) represents the glueball potential. We have higher glueball condensation when $G(r) \longrightarrow 0$, so it follows the same discussions as Figures 8 and 9. Also, an increase in quark mass m_q will lead to an increase in glueball condensation [198, 199]. We explored a phase transition from the low-energy IR regime to the high-energy UV regime by studying the characteristics of T_{c1} and T_{c2} in Equations (42) and (45) displayed in Figure 12. We find that the critical temperatures decrease with an increase in quark mass thereby increasing the strength of confinement. We observed that the light quarks that are confined in the IR regime $0 \le m_q \le 1$ are relegated to the QGP phase in the UV regime which confines quarks with $m_q > \sqrt{3}$. Finally, the chiral condensate $\langle \bar{q}q \rangle$ is calculated in Equation (85) and displayed in Figure 13.

The glueball condensation increases with an increase in depth of the curve. Hence, the condensate increases from $T = 0.9T_c$ (black), $T = 0.5$ (red), to $T = 0$ (blue).

As it is shown in Figure 2(a), the gradient of the graph increases with decreasing temperature from $T = 0.9T_c$ (black), $T = 0.5$ (red), to $T = 0$ (blue) [26, 93]. Within this temperature range, there is confinement and chiral symmetry breaking. In the right panel, we show how an increase in $m_q \longrightarrow \infty$ affects the behavior of the potential and confinement of the particles. As m_q is increasing, the potential increases and the confinement becomes stronger.

Here, we show the behavior of the string tension in the IR regime with varying temperatures. The string breaks quickly for light quarks while the heavier quarks have relatively longer life time even though they all vanish at $T = T_{c1}$. A regime is where all the bond states are expected to dissolve into a "soup" of their constituents. It also gives an insight into the behavior of the string tension for chiral limit $m_q = 0$ and chiral effective $m_q \neq 0$ regimes.

From Figure 4(a), the gradient of the curves decreases with increasing T from $T = 0$ (blue), $T = 0.5T_c$ (red), to $T = 0.9T_c$ (black), indicating a decrease in binding of the quarks as the energy of the system is increasing. At $T = T_c$ (dashed), we have

a deconfinement phase and restoration of the chiral symmetry [200, 201].

Figure 5 follows the same behavior as discussed in Figure 3. However, in this regime, the string breaking is explicit as the curves intercept the T/T_{c2} axis at different points. That notwithstanding, the bond states of the light and the heavy quarks will dissolve at $T = T_{c2}$. Also, the fluctuating glueball mass $m_s^2(T)$ in this regime is related to the string tension by $m_s(T) = \sqrt{3\sigma_s(T)}$.

Figure 7 is similar to Figure 2 for $m_q = 0$, $T = 0$ (blue), $T = 0.5T_c$ (red), and $T = 0.9T_c$ (black). This means that the gluons remain confined even if the quark mass is "removed" ($m_q = 0$) after confinement. This is known as *chromoelectric flux* confinement.

Confinement is stronger with increasing depth of the curves [18, 33]. Thus, the smaller the minima of the curves, the more condensed the glueballs and stronger the confinement. The minima increases from $T = 0$ (blue), $T = 0.5T_c$ (red), to $T = 0.9T_c$ (black).

The magnitude of the net potential decreases with increasing temperature, from $T = 0$ (blue), $T = 0.7T_c$ (red), to $T = 0.9T_c$ (black).

The condensation has its maximum value at $\bar{\eta} = 0$ and reduces steadily with increasing $\bar{\eta}$ until it vanishes.

The condensate reduces sharply with increasing temperature until it vanishes at $T = T_{c\eta}$.

We show a transition between the IR regime corresponding to lighter quark masses to the UV regime corresponding to heavier quark masses. The nonphysical behavior of T_{c1} at masses $m_q \leq 1$ is the regime where confinement of light quarks is observed in the IR regime. The curve becomes constant near $T_{c1} \simeq 1$, the point where the string tension in the IR regime gets saturated and begins to degenerate. Consequently, the IR regime can take masses within $0 \leq m_q \leq 1$; beyond this threshold, hadronization sets in and the string tension starts decaying. On the other hand, the UV regime takes in heavier quark masses (green curve), $m_q > \sqrt{3}$. The nonphysical behavior observed for $m_q \leq \sqrt{3}$ corresponds to the QGP regime with negative and constantly decaying σ_s. As m_q increases, T_{c2} decreases and the confinement becomes stronger.

An increase in quark mass courses the condensate to reduce sharply and eventually vanish at T/T_{cq} [153, 162]. This behavior is opposite to that of the string tension in Figures 3 and 5 as expected in QCD lattice simulations [202]. Consequently, confinement increases with increasing quark mass while the chiral condensate decreases with increasing quark mass.

6. Endnotes

[1]It is important to state at this point that the color dielectric function and the potential are related as $G(\phi) = (2\pi\alpha')^2 V(\phi)$ [203], where α' is the Regge slop with dimension of length squared. So, it absorbs the dimension of the potential rendering the $G(\phi)$ dimensionless. But we set $(2\pi\alpha') = 1$ throughout the paper for simplicity.

[2]This follows the Matsubara formalism of field theory at finite temperature where space time becomes topological. Here, one makes use of the Euclidean imaginary time and solve the path integral by imposing a periodic condition on the gauge field, $\omega_n = 2n\pi T$, and an antiperiodic condition, $\omega_n = (2n+1)\pi T$, for the fermion fields for $n \in \mathbb{Z}$. The imaginary time [204, 205] transforms as $\beta = 1/T$, where T is temperature.

[3]We used the standard integrals

$$\int_0^\infty \frac{x^3 dx}{e^x - 1} = \frac{\pi^4}{15}, \qquad \int_0^\infty \frac{x dx}{e^x - 1} = \frac{\pi^2}{6}. \tag{88}$$

[4]Here, we used

$$\int_0^\infty \frac{x dx}{e^x + 1} = \frac{\pi^2}{12}. \tag{89}$$

Data Availability

The data used to support the findings of this study are available from the corresponding author upon request.

Conflicts of Interest

The authors declare that they have no conflicts of interest.

Acknowledgments

We would like to thank CNPq, CAPES, and CNPq/PRONEX/FAPESQ-PB (Grant no. 165/2018), for partial financial support. FAB also acknowledges support from CNPq (Grant no. 312104/2018-9).

References

[1] S. Sarkar, H. Satz, and B. Sinha, "The physics of the quark-gluon plasma," *Lecture Notes in Physics*, vol. 785, no. 1, p. 369, 2010.

[2] PHENIX Collaboration, "J/ψ suppression at forward rapidity in Au + Au collisions at $\sqrt{s_{NN}}$=200 GeV," *Physical Review C*, vol. 84, article 054912, 2011.

[3] ATLAS Collaboration, "Measurement of the centrality dependence of J/ψ yields and observation of Z production in lead–lead collisions with the ATLAS detector at the LHC," *Physics Letters B*, vol. 697, no. 4, pp. 294–312, 2011.

[4] M. Asakawa and T. Hatsuda, "J/ψandηcin the deconfined plasma from lattice QCD," *Physical Review Letters*, vol. 92, no. 1, article 012001, 2004.

[5] T. Umeda, K. Nomura, and H. Matsufuru, "Charmonium at finite temperature in quenched lattice QCD," *European Physical Journal C: Particles and Fields*, vol. 39, no. 9, p. 26, 2005.

[6] S. Datta, F. Karsch, P. Petreczky, and I. Wetzorke, "Behavior of charmonium systems after deconfinement," *Physical Review D*, vol. 69, no. 9, article 094507, 2004.

[7] A. Jakovác, P. Petreczky, K. Petrov, and A. Velytsky, "Quarkonium correlators and spectral functions at zero and finite

temperature," *Physical Review D*, vol. 75, no. 1, article 014506, 2007.

[8] G. Aarts, C. Allton, M. B. Oktay, M. Peardon, and J. I. Skullerud, "Charmonium at high temperature in two-flavor QCD," *Physical Review D*, vol. 76, no. 9, article 094513, 2007.

[9] H. T. Ding, A. Francis, O. Kaczmarek, F. Karsch, H. Satz, and W. Söldner, "Charmonium correlation and spectral functions at finite temperature," *Proceedings of Science (Lattice)*, vol. 180, 2010.

[10] H. Ohno, S. Ejiri, S. Aoki et al., "Charmonium spectral functions with the variational method in zero and finite temperature lattice QCD," *Physical Review D*, vol. 84, no. 9, article 094504, 2011.

[11] T. Matsui and H. Satz, "J/ψ suppression by quark-gluon plasma formation," *Physics Letters B*, vol. 178, no. 4, pp. 416–422, 1986.

[12] S. Digal, P. Petreczky, and H. Satz, "String breaking and quarkonium dissociation at finite temperatures," *Physics Letters B*, vol. 514, no. 1-2, pp. 57–62, 2001.

[13] E. V. Shuryak and I. Zahed, "Toward a theory of binary bound states in the quark-gluon plasma," *Physical Review D*, vol. 70, no. 5, article 054507, 2004.

[14] D. Cabrera and R. Rapp, "*T*-matrix approach to quarkonium correlation functions in the quark-gluon plasma," *Physical Review D*, vol. 76, no. 11, article 114506, 2007.

[15] W. M. Alberico, A. Beraudo, A. De Pace, and A. Molinari, "Quarkonia in the deconfined phase: effective potentials and lattice correlators," *Physical Review D*, vol. 75, no. 7, article 074009, 2007.

[16] A. Mocsy and P. Petreczky, "Can quarkonia survive deconfinement?," *Physical Review D*, vol. 77, no. 1, article 014501, 2008.

[17] H. Iida, T. Doi, N. Ishii, H. Suganuma, and K. Tsumura, "Charmonium properties in deconfinement phase in anisotropic lattice QCD," *Physical Review D*, vol. 74, no. 7, article 074502, 2006.

[18] A. Issifu and F. A. Brito, "Confinement of fermions in tachyon matter," *Advances in High Energy Physics*, vol. 2020, Article ID 1852841, 18 pages, 2020.

[19] A. Issifu and F. A. Brito, "The (de)confinement transition in tachyonic matter at finite temperature," *Advances in High Energy Physics*, vol. 2019, Article ID 9450367, 9 pages, 2019.

[20] N. R. Soni, B. R. Joshi, R. P. Shah, H. R. Chauhan, and J. N. Pandya, "$Q\bar{Q}(Q \in \{b, c\})$ spectroscopy using the Cornell potential," *European Physical Journal C: Particles and Fields*, vol. 78, no. 7, 2018.

[21] E. Eichten, S. Godfrey, H. Mahlke, and J. L. Rosner, "Quarkonia and their transitions," *Reviews of Modern Physics*, vol. 80, no. 3, pp. 1161–1193, 2008.

[22] S. Godfrey and S. L. Olsen, "The exotic *XYZ* charmonium-like mesons," *Annual Review of Nuclear and Particle Science*, vol. 58, no. 1, pp. 51–73, 2008.

[23] T. Barnes and S. L. Olsen, "Chapter 14 charmonium spectroscopy," *International Journal of Modern Physics A: Particles and Fields; Gravitation; Cosmology; Nuclear Physics*, vol. 24, supplement 01, pp. 305–325, 2009.

[24] N. Brambilla, S. Eidelman, P. Foka et al., "QCD and strongly coupled gauge theories: challenges and perspectives," *European Physical Journal C: Particles and Fields*, vol. 74, no. 10, article 2981, 2014.

[25] A. Andronic, F. Arleo, R. Arnaldi et al., "Heavy-flavour and quarkonium production in the LHC era: from proton–proton to heavy-ion collisions," *European Physical Journal C: Particles and Fields*, vol. 76, no. 3, p. 107, 2016.

[26] N. Brambilla, S. Eidelman, B. K. Heltsley et al., "Heavy quarkonium: progress, puzzles, and opportunities," *European Physical Journal C: Particles and Fields*, vol. 71, no. 2, article 1534, 2011.

[27] A. Sen, "Stable non-BPS bound states of BPS D-branes," *Journal of High Energy Physics*, vol. 1998, no. 8, 1998.

[28] H. Boschi-Filho, N. R. F. Braga, and C. N. Ferreira, "Heavy quark potential at finite temperature from gauge-string duality," *Physical Review D*, vol. 74, no. 8, article 086001, 2006arXiv:hep-th/0607038.

[29] V. Vento, "Glueball-meson mixing," *European Physical Journal A: Hadrons and Nuclei*, vol. 52, no. 1, 2016.

[30] L. Burakovsky and P. R. Page, "Scalar glueball mixing and decay," *Physical Review D*, vol. 59, no. 1, article 014022, 1998arXiv:hep-ph/9807400.

[31] H. Genz, M. Nowakowski, and D. Woitschitzky, "Mixings of a pseudoscalar glueball," *Physics Letters B*, vol. 250, no. 1-2, pp. 143–150, 1990.

[32] Y. A. Simonov, "Mixing of meson, hybrid, and glueball states," *Physics of Atomic Nuclei*, vol. 64, no. 10, pp. 1876–1886, 2001.

[33] G. S. Bali, "QCD forces and heavy quark bound states," *Physics Reports*, vol. 343, no. 1-2, pp. 1–136, 2001.

[34] Particle Data Group, "Review of particle physics," *Physical Review D*, vol. 98, no. 3, article 030001, 2018and 2019 updated.

[35] J. Sonnenschein and D. Weissman, "Rotating strings confronting PDG mesons," *Journal of High Energy Physics*, vol. 2014, no. 8, p. 13, 2014.

[36] J. Sonnenschein and D. Weissman, "A rotating string model versus baryon spectra," *Journal of High Energy Physics*, vol. 2015, no. 2, p. 147, 2015.

[37] J. Sonnenschein and D. Weissman, "The decay width of stringy hadrons," *Nuclear Physics B*, vol. 927, no. 368, p. 454, 2018.

[38] S. Narison, "Light and heavy quark masses, test of PCAC and flavour breakings of condensates in QCD," *Physics Letters B*, vol. 216, no. 1-2, pp. 191–197, 1989.

[39] T. Hatsuda and T. Kunihiro, "QCD phenomenology based on a chiral effective Lagrangian," *Physics Reports*, vol. 247, no. 5-6, pp. 221–367, 1994.

[40] C. J. Morningstar and M. Peardon, "Glueball spectrum from an anisotropic lattice study," *Physical Review D*, vol. 60, no. 3, article 034509, 1999.

[41] M. Loan, X.-Q. Luo, and Z.-H. Luo, "Monte Carlo study of glueball masses in the Hamiltonian limit of SU(3) lattice gauge theory," *International Journal of Modern Physics A*, vol. 21, no. 13n14, pp. 2905–2936, 2006.

[42] Y. Chen, A. Alexandru, S. J. Dong et al., "Glueball spectrum and matrix elements on anisotropic lattices," *Physical Review D*, vol. 73, no. 1, article 014516, 2006.

[43] W. Lee and D. Weingarten, "Scalar quarkonium masses and mixing with the lightest scalar glueball," *Physical Review D*, vol. 61, no. 1, article 014015, 1999.

[44] G. S. Bali, A. Hulsebos, K. Schilling, A. C. Irving, C. Michael, and P. W. Stephenson, "A comprehensive lattice study of

SU(3) glueballs," *Physics Letters B*, vol. 309, no. 3-4, pp. 378–384, 1993.

[45] M. Albanese, G. Fiorentini, F. Costantini et al., "Glueball masses and string tension in lattice QCD," *Physics Letters B*, vol. 192, no. 1-2, pp. 163–169, 1987.

[46] P. Bacilieri, E. Remiddi, L. Fonti et al., "Scaling in lattice QCD: glueball masses and string tension," *Physics Letters B*, vol. 205, no. 4, pp. 535–539, 1988.

[47] M. Teper, "Glueballs, strings and topology in SU(N) gauge theory," *Nuclear Physics B - Proceedings Supplements*, vol. 109, no. 1, pp. 134–140, 2002.

[48] E. Eichten, K. Gottfried, T. Kinoshita, J. Kogut, K. D. Lane, and T.-M. Yan, "Spectrum of charmed quark-antiquark bound states," *Physical Review Letters*, vol. 34, no. 6, pp. 369–372, 1975.

[49] E. Eichten, K. Gottfried, T. Kinoshita, K. D. Lane, and T. M. Yan, "Charmonium: comparison with experiment," *Physical Review D*, vol. 21, no. 1, pp. 203–233, 1980.

[50] E. Eichten and F. Feinberg, "Spin-dependent forces in quantum chromodynamics," *Physical Review D*, vol. 23, no. 11, pp. 2724–2744, 1981.

[51] C. Quigg and J. L. Rosner, "Quantum mechanics with applications to quarkonium," *Physics Reports*, vol. 56, no. 4, pp. 167–235, 1979.

[52] T. Barnes, S. Godfrey, and E. S. Swanson, "Higher charmonia," *Physical Review D*, vol. 72, no. 5, article 054026, 2005.

[53] V. Sauli, "Bethe-Salpeter study of radially excited vector quarkonia," *Physical Review D*, vol. 86, no. 9, article 096004, 2012.

[54] S. Leitão, A. Stadler, M. T. Peña, and E. P. Biernat, "Linear confinement in momentum space: singularity-free bound-state equations," *Physical Review D*, vol. 90, no. 9, article 096003, 2014.

[55] S. Godfrey and N. Isgur, "Mesons in a relativized quark model with chromodynamics," *Physical Review D*, vol. 32, no. 1, pp. 189–231, 1985.

[56] S. Godfrey and K. Moats, "Bottomonium mesons and strategies for their observation," *Physical Review D*, vol. 92, no. 5, article 054034, 2015.

[57] S. Godfrey, "Spectroscopy of B_c mesons in the relativized quark model," *Physical Review D*, vol. 70, no. 5, article 054017, 2004.

[58] W.-J. Deng, H. Liu, L.-C. Gui, and X.-H. Zhong, "Charmonium spectrum and electromagnetic transitions with higher multipole contributions," *Physical Review D*, vol. 95, no. 3, article 034026, 2017.

[59] W.-J. Deng, H. Liu, L.-C. Gui, and X.-H. Zhong, "Spectrum and electromagnetic transitions of bottomonium," *Physical Review D*, vol. 95, no. 7, article 074002, 2017.

[60] A. P. Trawiński, S. D. Głazek, S. J. Brodsky, G. F. de Téramond, and H. G. Dosch, "Effective confining potentials for QCD," *Physical Review D*, vol. 90, no. 7, article 074017, 2014.

[61] R. Sundrum, "Hadronic string from confinement," 1997, https://arxiv.org/abs/hep-ph/9702306.

[62] J. J. Dudek, R. G. Edwards, N. Mathur, and D. G. Richards, "Charmonium excited state spectrum in lattice QCD," *Physical Review D*, vol. 77, no. 3, article 034501, 2008.

[63] S. Meinel, "Bottomonium spectrum from lattice QCD with 2 +1 flavors of domain wall fermions," *Physical Review D*, vol. 79, no. 9, article 094501, 2009.

[64] T. Burch, C. DeTar, M. di Pierro et al., "Quarkonium mass splittings in three-flavor lattice QCD," *Physical Review D*, vol. 81, no. 3, article 034508, 2010.

[65] For the Hadron Spectrum collaboration, L. Liu, G. Moir et al., "Excited and exotic charmonium spectroscopy from lattice QCD," *Journal of High Energy Physics*, vol. 2012, no. 7, article 126, 2012.

[66] C. McNeile, C. T. H. Davies, E. Follana, K. Hornbostel, G. P. Lepage, and HPQCD Collaboration, "Heavy meson masses and decay constants from relativistic heavy quarks in full lattice QCD," *Physical Review D*, vol. 86, no. 7, article 074503, 2012.

[67] J. O. Daldrop, C. T. H. Davies, R. J. Dowdall, and HPQCD Collaboration, "Prediction of the bottomoniumD-wave spectrum from full lattice QCD," *Physical Review Letters*, vol. 108, no. 10, article 102003, 2012.

[68] T. Kawanai and S. Sasaki, "Heavy quarkonium potential from Bethe-Salpeter wave function on the lattice," *Physical Review D*, vol. 89, no. 5, article 054507, 2014.

[69] T. Kawanai and S. Sasaki, "Interquark potential with finite quark mass from lattice QCD," *Physical Review Letters*, vol. 107, no. 9, article 091601, 2011.

[70] Y. Burnier, O. Kaczmarek, and A. Rothkopf, "Quarkonium at finite temperature: towards realistic phenomenology from first principles," *Journal of High Energy Physics*, vol. 2015, no. 12, pp. 1–34, 2015.

[71] Y. Burnier, O. Kaczmarek, and A. Rothkopf, "In-medium P-wave quarkonium from the complex lattice QCD potential," *Journal of High Energy Physics*, vol. 10, pp. 32–34, 2016.

[72] M. Kalinowski and M. Wagner, "Masses of D mesons, D_s mesons, and charmonium states from twisted-mass lattice QCD," *Physical Review D*, vol. 92, no. 9, article 094508, 2015.

[73] G. S. Bali, B. Bolder, N. Eicker et al., "Static potentials and glueball masses from QCD simulations with Wilson sea quarks," *Physical Review D*, vol. 62, no. 5, article 054503, 2000.

[74] C. Alexandrou, P. de Forcrand, and O. Jahn, "The ground state of three quarks," *Nuclear Physics B - Proceedings Supplements*, vol. 119, pp. 667–669, 2003.

[75] D. B. Lichtenberg, "Energy levels of quarkonia in potential models," *International Journal of Modern Physics A: Particles and Fields; Gravitation; Cosmology; Nuclear Physics*, vol. 2, no. 6, pp. 1669–1705, 1987.

[76] C. Corianó and H.-N. Li, "The transition to perturbative QCD in Compton scattering," *Nuclear Physics B*, vol. 434, no. 3, pp. 535–564, 1995.

[77] C. Corianó, H.-N. Li, and C. Savkli, "Exclusive QCD processes, quark-hadron duality, and the transition to perturbative QCD," *Journal of High Energy Physics*, vol. 1998, no. 7, 1998.

[78] V. A. Nesterenko and A. V. Radyushkin, "Sum rules and the pion form factor in QCD," *Physics Letters B*, vol. 115, no. 5, pp. 410–414, 1982.

[79] B. L. Ioffe and A. V. Smilga, "Pion formfactor at intermediate momentum transfer in QCD," *Physics Letters B*, vol. 114, no. 5, pp. 353–358, 1982.

[80] M. A. Shifman, A. I. Vainshtein, and V. I. Zakharov, "QCD and resonance physics. Theoretical foundations," *Nuclear Physics B*, vol. 147, no. 5, pp. 385–447, 1979.

[81] C. Corianó and H.-n. Li, "Stability analysis of sum rules for pion Compton scattering," *Physics Letters B*, vol. 324, no. 1, pp. 98–104, 1994.

[82] L. J. Reinders, H. Rubinstein, and S. Yazaki, "Hadron properties from QCD sum rules," *Physics Reports*, vol. 127, no. 1, pp. 1–97, 1985.

[83] P. Colangelo and A. Khodjamirian, "QCD sum rules, a modern perspective," 2001, https://www.worldscientific.com/doi/abs/10.1142/9789812810458_0033.

[84] G. W. Carter, O. Scavenius, I. N. Mishustin, and P. J. Ellis, "Effective model for hot gluodynamics," *Physical Review C*, vol. 61, no. 4, article 045206, 2000.

[85] D. E. Miller, "Gluon condensates at finite temperature," 2001, https://arxiv.org/abs/hep-ph/0008031.

[86] D. E. Miller, "Lattice QCD calculation for the physical equation of state," *Physics Reports*, vol. 443, no. 55, p. 96, 2007.

[87] D.-P. Min and N. Kochelev, "Glueball-induced partonic energy loss in quark-gluon plasma," *Physical Review C*, vol. 77, no. 1, article 014901, 2008.

[88] P. Bicudo, N. Cardoso, O. Oliveira, and P. J. Silva, "String tension at finite temperature lattice QCD," *Proceedings of Science (Lattice)*, vol. 300, 2011.

[89] O. Kaczmarek, F. Karsch, E. Laermann, and M. Lutgemeier, "Heavy quark potentials in quenched QCD at high temperature," *Physical Review D*, vol. 62, no. 3, article 034021, 2000.

[90] P. Petreczky, "Heavy quark potentials and quarkonium binding," *European Physical Journal C: Particles and Fields*, vol. 43, no. 1-4, pp. 51–57, 2005.

[91] N. Kochelev and D.-P. Min, "Role of glueballs in nonperturbative quark–gluon plasma," *Physics Letters B*, vol. 650, no. 239, p. 243, 2007.

[92] K. Yagi, T. Hatsuda, and Y. Miake, *Quark-gluon plasma: from big bang to little bang*, Cambridge University Press, Cambridge, UK, 2005.

[93] R. Pasechnik and M. Šumbera, "Phenomenological review on quark–gluon plasma: concepts vs. observations," *Universe*, vol. 3, no. 1, 2017.

[94] S. H. Lee, K. Morita, T. Song, and C. M. Ko, "Free energy versus internal energy potential for heavy-quark systems at finite temperature," *Physical Review D*, vol. 89, no. 9, article 094015, 2014.

[95] A. Mocsy and P. Petreczky, "Color screening melts quarkonium," *Physical Review Letters*, vol. 99, no. 21, article 211602, 2007.

[96] P. Gubler, K. Morita, and M. Oka, "Charmonium spectra at finite temperature from QCD sum rules with the maximum entropy method," *Physical Review Letters*, vol. 107, no. 9, article 092003, 2011.

[97] H.-T. Ding, A. Francis, O. Kaczmarek, F. Karsch, H. Satz, and W. Soeldner, "Charmonium properties in hot quenched lattice QCD," *Physical Review D*, vol. 86, no. 1, article 014509, 2012.

[98] T. J. Allen, T. Coleman, M. G. Olsson, and S. Veseli, "QCD string structure in vector confinement," *Physical Review D*, vol. 67, no. 5, article 054016, 2003.

[99] J. Franklin, "A simple Dirac wave function for a coulomb potential with linear confinement," *Modern Physics Letters A*, vol. 14, no. 34, pp. 2409–2411, 1999.

[100] A. S. De Castro and J. Franklin, "Exact solutions of the Dirac equation for modified coulombic potentials," *International Journal of Modern Physics A: Particles and Fields; Gravitation; Cosmology; Nuclear Physics*, vol. 15, no. 27, pp. 4355–4360, 2000.

[101] H. W. Crater, J.-H. Yoon, and C.-Y. Wong, "Singularity structures in Coulomb-type potentials in two-body Dirac equations of constraint dynamics," *Physical Review D*, vol. 79, no. 3, article 034011, 2009.

[102] R. Dick, "Vector and scalar confinement in gauge theory with a dilaton," *Physics Letters B*, vol. 409, no. 1-4, pp. 321–324, 1997.

[103] L. Cao, Y.-C. Yang, and H. Chen, "Charmonium states in QCD-inspired quark potential model using Gaussian expansion method," *Few-Body Systems*, vol. 53, no. 3-4, pp. 327–342, 2012.

[104] T. Schäfer and E. Shuryak, "Instantons in QCD," *Reviews of Modern Physics*, vol. 70, no. 2, pp. 323–425, 1998.

[105] A. Deur, "Study of spin sum rules (and the strong coupling constant at large distances)," 2009, https://arxiv.org/abs/0907.3385.

[106] V. I. Zakharov, "Gluon condensate and beyond," *International Journal of Modern Physics A: Particles and Fields; Gravitation; Cosmology; Nuclear Physics*, vol. 14, no. 31, pp. 4865–4879, 1999.

[107] H.-B. Tang and R. J. Furnstahl, "The gluon condensate and running coupling of QCD," 1995, https://arxiv.org/abs/hep-ph/9502326.

[108] K.-I. Kondo, "Vacuum condensates, effective gluon mass and color confinement in a new reformulation of QCD," 2003, https://arxiv.org/abs/hep-th/0307270.

[109] K.-I. Kondo, "Vacuum condensates, effective gluon mass and color confinement," 2004, https://arxiv.org/abs/hep-th/0311033.

[110] J. M. Cornwall and A. Soni, "Glueballs as bound states of massive gluons," *Physics Letters B*, vol. 120, no. 4-6, pp. 431–435, 1983.

[111] E. V. Gorbar and A. A. Natale, "Relating the quark and gluon condensates through the QCD vacuum energy," *Physical Review D*, vol. 61, no. 5, article 054012, 2000.

[112] R. Fukuda, "Gluon condensation and the properties of the vacuum in quantum chromodynamics," *Progress in Theoretical Physics*, vol. 67, no. 2, pp. 648–654, 1982.

[113] H. Kohyama, "Effective model based on QCD with gluon condensate," 2016, https://arxiv.org/abs/1606.00673.

[114] D. B. Leinweber, J. I. Skullerud, A. G. Williams, and C. Parrinello, "Asymptotic scaling and infrared behavior of the gluon propagator," *Physical Review D*, vol. 60, no. 9, article 094507, 1999.

[115] K. Langfeld, H. Reinhardt, and J. Gattnar, "Gluon propagator and quark confinement," *Nuclear Physics B*, vol. 621, no. 1-2, pp. 131–156, 2002.

[116] C. Alexandrou, P. de Forcrand, and E. Follana, "Gluon propagator without lattice Gribov copies on a finer lattice," *Physical Review D*, vol. 65, no. 11, article 114508, 2002.

[117] J. H. Field, "Phenomenological analysis of gluon mass effects in inclusive radiative decays of theJ/ψandΥ," *Physical Review D*, vol. 66, no. 1, article 013013, 2002.

[118] M. Consoli and J. H. Field, "Effective gluon mass and the determination of α_s from J/ψ and Υ branching ratios," *Physical Review D*, vol. 49, no. 3, pp. 1293–1301, 1994.

[119] I. I. Kogan and A. Kovner, "Variational approach to the QCD wave functional: dynamical mass generation and confinement," *Physical Review D*, vol. 52, no. 6, pp. 3719–3734, 1995.

[120] D. Diakonov, "Instantons at work," *Progress in Particle and Nuclear Physics*, vol. 51, no. 1, pp. 173–222, 2003.

[121] D. Diakonov, "Topology and confinement," *Nuclear Physics B-Proceedings Supplements*, vol. 195, pp. 5–45, 2009.

[122] P. J. Silva, O. Oliveira, P. Bicudo, and N. Cardoso, "Gluon screening mass at finite temperature from the Landau gauge gluon propagator in lattice QCD," *Physical Review D*, vol. 89, no. 7, article 074503, 2014.

[123] J. C. Collins and M. J. Perry, "Superdense matter: neutrons or asymptotically free quarks?," *Physical Review Letters*, vol. 34, no. 21, pp. 1353–1356, 1975.

[124] N. Cabibbo and G. Parisi, "Exponential hadronic spectrum and quark liberation," *Physics Letters B*, vol. 59, no. 1, pp. 67–69, 1975.

[125] D. J. Gross and F. Wilczek, "Ultraviolet behavior of non-Abelian gauge theories," *Physical Review Letters*, vol. 30, no. 26, pp. 1343–1346, 1973.

[126] H. D. Politzer, "Reliable perturbative results for strong interactions?," *Physical Review Letters*, vol. 30, no. 26, pp. 1346–1349, 1973.

[127] H. Fritzsch, M. Gell-Mann, and H. Leutwyler, "Advantages of the color octet gluon picture," *Physics Letters B*, vol. 47, no. 4, pp. 365–368, 1973.

[128] A. D. Linde, "Phase transitions in gauge theories and cosmology," *Reports on Progress in Physics*, vol. 42, no. 3, pp. 389–437, 1979.

[129] D. Bailin and A. Love, *Cosmology in Gauge Field Theory and String Theory*, IOP, Bristol, UK, 2004.

[130] D. Boyanovsky, H. J. de Vega, and D. J. Schwarz, "Phase transitions in the early and present universe," *Annual Review of Nuclear and Particle Science*, vol. 56, no. 1, pp. 441–500, 2006.

[131] M. Trodden, "Electroweak baryogenesis," *Reviews of Modern Physics*, vol. 71, no. 5, pp. 1463–1500, 1999.

[132] K. Kajantie, M. Laine, K. Rummukainen, and M. Shaposhnikov, "Is there a hot electroweak phase transition at $m_H \gtrsim m_W$?," *Physical Review Letters*, vol. 77, no. 14, pp. 2887–2890, 1996.

[133] L. Susskind, "Lattice models of quark confinement at high temperature," *Physical Review D*, vol. 20, no. 10, pp. 2610–2618, 1979.

[134] P. Petreczky, "Lattice QCD at non-zero temperature," *Journal of Physics G: Nuclear and Particle Physics*, vol. 39, no. 9, article 093002, 2012.

[135] STAR Collaboration, "Experimental and theoretical challenges in the search for the quark–gluon plasma: the STAR Collaboration's critical assessment of the evidence from RHIC collisions," *Nuclear Physics A*, vol. 757, no. 1-2, pp. 102–183, 2005.

[136] Y. Aoki, G. Endrődi, Z. Fodor, S. D. Katz, and K. K. Szabó, "The order of the quantum chromodynamics transition predicted by the standard model of particle physics," *Nature*, vol. 443, no. 7112, pp. 675–678, 2006.

[137] T. Bhattacharya, M. I. Buchoff, N. H. Christ et al., "QCD phase transition with chiral quarks and physical quark masses," *Physical Review Letters*, vol. 113, no. 8, article 082001, 2014.

[138] M. Cheng, N. H. Christ, S. Datta et al., "QCD equation of state with almost physical quark masses," *Physical Review D*, vol. 77, no. 1, article 014511, 2008.

[139] J.-P. Blaizot, E. Iancu, and A. Rebhan, "Thermodynamics of the high-temperature quark-gluon plasma," 2003, https://arxiv.org/abs/hep-ph/0303185.

[140] K. Kajantie, M. Laine, J. Peisa, A. Rajantie, K. Rummukainen, and M. Shaposhnikov, "Nonperturbative Debye mass in finite temperature QCD," *Physical Review Letters*, vol. 79, no. 17, pp. 3130–3133, 1997.

[141] S. Nadkarni, "Non-Abelian Debye screening: the color-averaged potential," *Physical Review D*, vol. 33, no. 12, pp. 3738–3746, 1986.

[142] E. Manousakis and J. Polonyi, "Nonperturbative length scale in high-temperature QCD," *Physical Review Letters*, vol. 58, no. 9, pp. 847–850, 1987.

[143] D. S. Kuzmenko, I. Shevchenko, and Y. A. Simonov, "The QCD vacuum, confinement and strings in the vacuum correlator method," 2003, https://arxiv.org/abs/hep-ph/0310190.

[144] Y. A. Simonov, "The confinement," *Physics-Uspekhi*, vol. 39, no. 4, pp. 313–336, 1996.

[145] H. G. Dosch, "Gluon condensate and effective linear potential," *Physics Letters B*, vol. 190, no. 1-2, pp. 177–181, 1987.

[146] H. G. Dosch and Y. A. Simonov, "The area law of the Wilson loop and vacuum field correlators," *Physics Letters B*, vol. 205, no. 2-3, pp. 339–344, 1988.

[147] Y. A. Simonov, "Vacuum background fields in QCD as a source of confinement," *Nuclear Physics B*, vol. 307, no. 3, pp. 512–530, 1988.

[148] A. di Giacomo, H. G. Dosch, V. I. Shevchenko, and Y. A. Simonov, "Field correlators in QCD. Theory and applications," *Physics Reports*, vol. 372, no. 4, pp. 319–368, 2002.

[149] P. Bicudo and G. M. Marques, "Chiral symmetry breaking and scalar string confinement," *Physical Review D*, vol. 70, no. 9, article 094047, 2004.

[150] R. Kitano, "Hidden local symmetry and color confinement," 2011, https://arxiv.org/abs/1109.6158.

[151] H. Suganuma, S. Sasaki, and H. Toki, "Color confinement, quark pair creation and dynamical chiral-symmetry breaking in the dual Ginzburg-Landau theory," *Nuclear Physics B*, vol. 435, no. 1-2, pp. 207–240, 1995.

[152] S. Weinberg, *The Quantum Theory of Fields. Vol. 2: Modern Applications*, Cambridge University Press, 1996.

[153] S. Borsanyi, Z. Fodor, C. Hoelbling et al., "Is there still any T_c mystery in lattice QCD? Results with physical masses in the continuum limit III," *Journal of High Energy Physics*, vol. 9, 2010.

[154] A. Bazavov, T. Bhattacharya, M. Cheng et al., "Equation of state and QCD transition at finite temperature," *Physical Review D*, vol. 80, no. 1, article 014504, 2009.

[155] B. Borasoy and U.-G. Meissner, "Chiral expansion of baryon masses andσ-terms," *Annals of Physics*, vol. 254, no. 1, pp. 192–232, 1997.

[156] S. Durr, Z. Fodor, J. Frison et al., "Ab initio determination of light hadron masses," *Science*, vol. 322, no. 5905, pp. 1224–1227, 2008.

[157] A. Höll, P. Maris, C. D. Roberts, and S. V. Wright, "Schwinger functions, light-quark bound states and sigma terms," *Nuclear Physics B - Proceedings Supplements*, vol. 161, pp. 87–94, 2006.

[158] V. V. Flambaum, A. Höll, P. Jaikumar, C. D. Roberts, and S. V. Wright, "Sigma terms of light-quark hadrons," *Few-Body Systems*, vol. 38, no. 1, pp. 31–51, 2006.

[159] H. Leutwyler, "On the foundations of chiral perturbation theory," *Annals of Physics*, vol. 235, no. 1, pp. 165–203, 1994.

[160] J. J. M. Verbaarschot and T. Wettig, "Random matrix theory and chiral symmetry in QCD," *Annual Review of Nuclear and Particle Science*, vol. 50, no. 1, pp. 343–410, 2000.

[161] V. Koch, "Aspects of chiral symmetry," *International Journal of Modern Physics E: Nuclear Physics*, vol. 6, no. 2, pp. 203–249, 1997.

[162] J. Jankowski, D. Blaschke, and M. Spalinski, "Chiral condensate in hadronic matter," 2013, https://arxiv.org/abs/1212.5521.

[163] R. Dashen, S. Ma, and H. J. Bernstein, "S-matrix formulation of statistical mechanics," *Physical Review A*, vol. 6, no. 2, p. 851, 1972.

[164] G. 't Hooft, C. Itzykson, A. Jaffe et al., *Recent developments in gauge theories*, vol. 59 of NATO Advanced Study Institutes Series, Springer, Boston, MA, USA, 1980.

[165] S. R. Coleman, "Secret symmetry: an introduction to spontaneous symmetry breakdown and gauge fields," *The Subnuclear Series*, vol. 11, p. 139, 1975.

[166] S. Fiorilla, N. Kaiser, and W. Weise, "Thermodynamics of the in-medium chiral condensate," 2011, https://arxiv.org/abs/1104.2819.

[167] J. T. Lenaghan, D. H. Rischke, and J. Schaffner-Bielich, "Chiral symmetry restoration at nonzero temperature in the $SU(3)_r \times SU(3)_l$ linear sigma model," *Physical Review D*, vol. 62, no. 8, article 085008, 2000.

[168] P. D. B. Collins, A. D. Martin, and E. J. Squires, *Particle Physics and Cosmology*, John Wiley & Sons, Inc., Canada, 1989.

[169] B. Mohanty and J. Serreau, "Disoriented chiral condensate: theory and experiment," *Physics Reports*, vol. 414, no. 6, pp. 263–358, 2005.

[170] J. D. Bjorken, *What lies ahead?*, SLAC-PUB-5673, 1991.

[171] J.-P. Blaizot and A. Krzywicki, "Soft-pion emission in high-energy heavy-ion collisions," *Physical Review D*, vol. 46, no. 1, pp. 246–251, 1992.

[172] A. E. Nelson and D. B. Kaplan, "Strange condensate realignment in relativistic heavy ion collisions," *Physics Letters B*, vol. 192, no. 1-2, pp. 193–197, 1987.

[173] A. A. Anselm, "Classical states of the chiral field and nuclear collisions at very high energy," *Physics Letters B*, vol. 217, no. 1-2, pp. 169–172, 1989.

[174] A. A. Anselm and M. G. Ryskin, "Production of classical pion field in heavy ion high energy collisions," *Physics Letters B*, vol. 266, no. 3-4, pp. 482–484, 1991.

[175] C. M. G. Lattes, Y. Fujimoto, and S. Hasegawa, "Hadronic interactions of high energy cosmic-ray observed by emulsion chambers," *Physics Reports*, vol. 65, no. 3, pp. 151–229, 1980.

[176] C. R. A. Augusto, S. L. C. Barroso, V. Kopenkin, M. Moriya, C. E. Navia, and E. H. Shibuya, "Search for disoriented chiral condensate in cosmicγ-hadron families," *Physical Review D*, vol. 59, no. 5, article 054001, 1999.

[177] E. G. Dziadus, "Are Centauros exotic signals of the QGP?," *Physics of Particles and Nuclei*, vol. 34, pp. 285–347, 2003, (Fiz. Elem. Chast. Atom. Yadra 34, 565 678,(2003)) arXiv:-hep-ph/0111163.

[178] K. Rajagopal and F. Wilczek, "Static and dynamic critical phenomena at a second order QCD phase transition," *Nuclear Physics B*, vol. 399, no. 2-3, pp. 395–425, 1993.

[179] K. Rajagopal and F. Wilczek, "Emergence of coherent long wavelength oscillations after a quench: application to QCD," *Nuclear Physics B*, vol. 404, pp. 577–589, 1993.

[180] UAl Collaboration, "Search for centauro like events at the CERN proton-antiproton collider," *Physics Letters B*, vol. 122, no. 2, pp. 189–196, 1983.

[181] UA5 Collaboration, "Production of photons and search for Centauro events at the SPS collider," *Physics Letters B*, vol. 115, no. 1, pp. 71–76, 1982.

[182] UA5 Collaboration, "An accelerator search at 900 GeV CM energy for the Centauro phenomenon," *Physics Letters B*, vol. 180, no. 4, pp. 415–422, 1986.

[183] CDF Collaboration, "Search for Centauro events at CDF," in *XIth Topical Workshop on ppbar Collider Physics*, Abano Terme (Padova), Italy, July 1996.

[184] MiniMax Collaboration, "Search for disoriented chiral condensate at the Fermilab Tevatron," *Physical Review D*, vol. 61, article 032003, 2000.

[185] WA98 Collaboration, "Search for disoriented chiral condensates in 158 AGeV Pb+Pb collisions," *Physics Letters B*, vol. 420, no. 1-2, pp. 169–179, 1998.

[186] WA98 Collaboration, "Localized charged-neutral fluctuations in 158A GeV Pb+Pb collisions," *Physical Review C*, vol. 64, article 011901, 2001.

[187] WA98 Collaboration, "Centrality dependence of charged-neutral particle fluctuations in 158A GeV ^{208}Pb+^{208}PB collisions," *Physical Review C*, vol. 67, article 044901, 2003.

[188] NA49 collaboration, "Event-by-event fluctuations of average transverse momentum in central Pb+ Pb collisions at 158 GeV per nucleon," *Physics Letters B*, vol. 459, pp. 679–686, 1999.

[189] T. Nakamura, K. Homma, and PHENIX Collaboration, *Study of Isospin Fluctuations at RHIC-PHENIX*, Quark Matter, Nantes, France, 2002.

[190] STAR Collaboration, "STAR detector overview," *Nuclear Instruments and Methods in Physics Research Section A: Accelerators, Spectrometers, Detectors and Associated Equipment*, vol. 499, pp. 624–632, 2003.

[191] ALICE Collaboration, *Technical Proposal for a Large Ion Collider Experiment at the CERN LHC*, CERN-LHCC-95-71, CERN-LHCC-P-3, 1995.

[192] A. L. S. Angelis, X. Aslanoglou, J. Bartke et al., "Formation of Centauro in Pb+Pb collisions at the LHC and their detection with the CASTOR detector of CMS," *Nuclear Physics B*, vol. 122, no. 205, pp. 205–208, 2003.

[193] H. Boschi-Filho, N. R. F. Braga, and C. N. Ferreira, "Static strings in Randall-Sundrum scenarios and the quark-antiquark potential," *Physical Review D*, vol. 73, no. 10, article 106006, 2006.

[194] R. D. Pisarski and O. Alvarez, "Strings at finite temperature and deconfinement," *Physical Review D*, vol. 26, no. 12, pp. 3735–3737, 1982.

[195] P. De Forcrand, G. Schierholz, H. Schneider, and M. Teper, "The string and its tension in Su(3) lattice gauge theory: towards definitive results," *Physics Letters B*, vol. 160, no. 1-3, pp. 137–143, 1985.

[196] K. Fukushima, "Chiral effective model with the Polyakov loop," *Physics Letters B*, vol. 591, no. 3-4, pp. 277–284, 2004.

[197] M. Cheng, N. H. Christ, S. Datta et al., "Transition temperature in QCD," *Physical Review D*, vol. 74, no. 5, article 054507, 2006.

[198] A. Sen, "Tachyon matter," *Journal of High Energy Physics*, vol. 2002, no. 7, p. 65, 2002.

[199] A. Sen, "Rolling tachyon," *Journal of High Energy Physics*, vol. 2002, no. 4, p. 48, 2002.

[200] R. Gupta, G. Guralnik, G. W. Kilcup, A. Patel, and S. R. Sharpe, "Clear evidence for a first-order chiral transition in QCD," *Physical Review Letters*, vol. 57, no. 21, pp. 2621–2624, 1986.

[201] S. Gottlieb, W. Liu, D. Toussaint, R. L. Renken, and R. L. Sugar, "Chiral-symmetry breaking in lattice QCD with two and four fermion flavors," *Physical Review D*, vol. 35, no. 12, pp. 3972–3980, 1987.

[202] C. Schmidt, T. Umeda, and for the RBC-Bielefeld Collaboration, "Thermodynamics of (2+1)-flavor QCD," *Nuclear Physics A*, vol. 785, no. 1-2, pp. 274–277, 2007.

[203] M. R. Garousi, "Tachyon couplings on non-BPS D-branes and Dirac–Born–Infeld action," *Nuclear Physics B*, vol. 584, no. 1-2, pp. 284–299, 2000.

[204] N. P. Landsman and C. G. van Weert, "Real- and imaginary-time field theory at finite temperature and density," *Physics Reports*, vol. 145, no. 3-4, pp. 141–249, 1987.

[205] E. Megías, E. Ruiz Arriola, and L. L. Salcedo, "Polyakov loop in chiral quark models at finite temperature," *Physical Review D*, vol. 74, no. 6, article 065005, 2006.